Table 2 Correlation between the expression of ShcC protein and identified prognostic factors of neuroblastoma

	p52		*p67*	
	Average	*t-Test*	*Average*	*t-Test*
ShcC				
Age (months)				
12 >	0.071		0.037	
> 12	0.27	**<0.001**	0.18	0.015
Stage				
I–II	0.03		0.0084	
III–IV	0.26	**<0.001**	0.14	**<0.001**
MYCN				
Single	0.083		0.040	
amp.	0.43	**0.002**	0.25	**0.005**
Death in 12 months				
–	0.10		0.047	
+	0.41	**0.006**	0.25	**0.009**
	p52		*p66*	
	Average	*t-Test*	*Average*	*t-Test*
ShcA				
Age (months)				
12 >	0.72		0.53	
> 12	0.82	0.2	0.52	0.32
Stage				
I–II	0.68		0.52	
III–IV	0.82	0.1	0.52	0.22
MYCN				
Single	0.73		0.51	
amp.	0.88	0.16	0.55	0.16
Death in 12 months				
–	0.75		0.50	
+	0.84	0.27	0.57	0.11

Expression levels of ShcC and ShcA in tissue samples from 46 neuroblastoma patients quantified were analyzed statistically using *t*-test. The variables compared are age, onset of the disease (months); stage, INSS stage; MYCN, single copy or amplification of *MYCN* gene. Statistically significant correlation ($P<0.01$) is indicated in bold.

cells were plated on collagen dishes following suspending condition (Figure 4a, lower panel). On the contrary, the activation level of ERK due to ShcC RNAi was not significant in the suspending condition (Supplementary Figure E, left panel) showing that ShcC RNAi-induced ERK activation depends on attachment to the specific extracellular matrix (ECM).

In contrast, ERK activation was consistently suppressed by knockdown of ShcA regardless of these culture conditions (Figure 4a, upper panel).

Integrins-mediated extracellular signaling lead the activation of Ras/ERK signaling by ShcA, and that process is reported to be associated with Src family kinase (Wary *et al*., 1996, 1998), focal adhesion kinase (Hecker *et al*., 2002) or some RTKs (Moro *et al*., 1998; Hinsby *et al*., 2004). In TNB-1 cells, enhanced ShcA phosphorylation and ShcA–Grb2 complex formation was observed following collagen stimulation and further increased by ShcC RNAi (Figures 4b and c). To examine whether the phosphorylation of ShcA is necessary for the neurite formation, the effect of double knockdown of both ShcC and ShcA was examined in TNB-1 cells. ERK activation and neurite outgrowth were not detected in the absence of both ShcC and ShcA, indicating that ShcC RNAi-induced neurite outgrowth of TNB-1 cells might be dependent on the ShcA expression in adherent state (Figure 4d).

Expression of ShcC suppresses the phosphorylation of ShcA in KU-YS cells stimulated by EGF

To further analyse the effects of ShcC expression on ShcA phosphorylation in neuroblastoma cells, we introduced a vector expressing p52ShcC into KU-YS neuroblastoma cells, which do not express a detectable amount of endogenous ShcC protein (Figure 1A), and obtained several stable clones expressing p52ShcC at different levels (Figure 5a). As controls, clones overexpressing p46/p52ShcA, or expressing the expression vector alone were also prepared. We checked the ShcA phosphorylation of each clone under the stimulation of EGF (Figure 5b). EGF stimulation to the control and ShcA expressing cells showed typical activation of ShcA, whereas the cell expressing ShcC showed decreased levels of ShcA phosphorylation according to the levels of ShcC protein. We also confirmed that activation of ShcA by EGF was suppressed in the cells transiently overexpressing ShcC (Supplementary Figure F). Those cells showed almost the same level of EGF receptor (EGFR) activation induced by EGF, judging from the phosphorylation levels of EGFR indicating that the expression of ShcC negatively affected the EGFR–ShcA signaling after the activation of EGFR, such as competing manners against ShcA. In addition, we examined whether tyrosine phosphorylation of ShcC is crucial for the suppression of ShcA phosphorylation by establishing two clones that express a p52ShcC mutant, 3YF lacking all three tyrosines, which are reported to be involved in the tyrosine phosphorylation of ShcC (Miyake *et al*., 2005). It was revealed that the 3YF mutant of ShcC could suppress the EGF-induced activation of ShcA in both clones almost as efficiently as the original ShcC in ShcC2 cells (Supplementary Figure G), suggesting that negative regulation of ShcA phosphorylation by ShcC does not require tyrosine phosphorylation of ShcC.

ShcC downregulation negatively affects anchorage-independent growth and in vivo *tumorigenicity*

We investigated the effect of ShcC knockdown on the anchorage-independent growth and *in vivo* tumorigenicity of TNB-1 cells by establishing cells with stable suppression of ShcC expression using the miR RNAi expression vector (as described in 'Materials and methods'). As analysed in the mixed clones by soft agar colony formation assay, stable suppression of ShcC caused marked inhibition of anchorage-independent growth (Figure 6a). Three isolated clones of ShcC miR

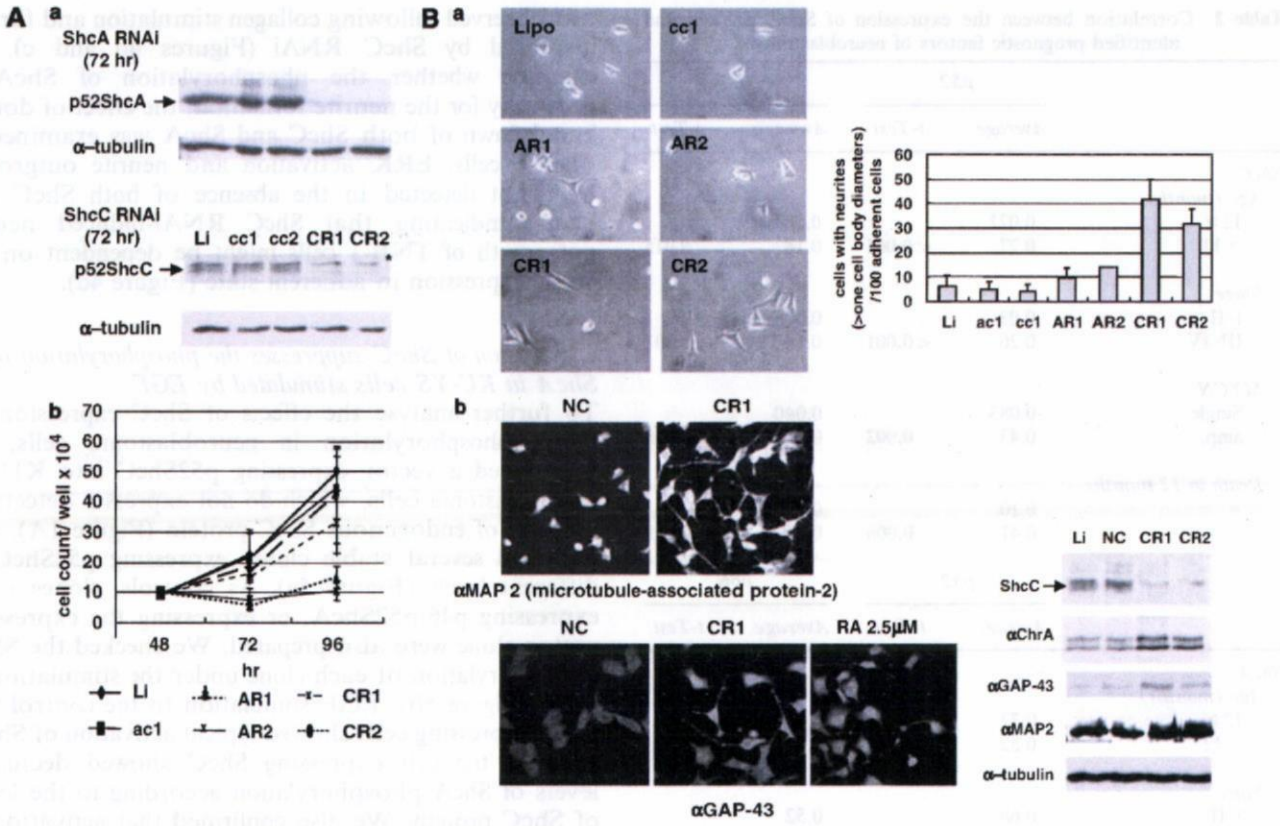

Figure 2 Biological effects of ShcC downregulation using small interfering RNA (siRNA) on TNB-1 cells. (**A**) (a) Expression of ShcC (lower panel) and ShcA (upper panel) was suppressed by RNA interference using specific siRNA oligonucleotides corresponding to ShcC and ShcA, respectively, then, detected by western analysis with each specific antibody. (b) Growth rate of siRNA-treated cells in tissue culture condition. TNB-1 cells 48 h after the transfection with ShcA/ShcC siRNA cultured by 30-mm dishes were counted at the indicated time points. The results represent the average values (±s.d.) of three replicated experiments. (**B**) Downregulation of ShcC induces neurite outgrowth and increases the expression of differentiation-related markers in TNB-1 cells. (a) Evaluation of neurite outgrowth of ShcA or ShcC-knockdown TNB-1 cells 72 h after siRNA treatment without any extracellular matrix (ECM) stimulation. (b) Expression of several molecules used as differentiation-related markers in ShcC-knockdown TNB-1 cells (left panel: immunostaining of neuritis as described in 'Materials and methods'; right panel: western analysis using indicated antibodies). As a positive control of differentiation, 2.5 μM retinoic acid (RA) was treated 24 h before analysis. AR1, AR2/CR1, CR2: two independent siRNA of ShcA /ShcC; Li: treated with only Lipofectamine 2000; ac1, ac2/cc1, cc2: control siRNA for ShcA /ShcC siRNA, respectively. NC: negative control for universal siRNA (as described in 'Materials and methods').

RNAi (miShcC-1, -2 and -3) were prepared by checking the level of ShcC protein along with clones of LacZ miR RNAi (miLacZ-1 and -2) as controls (Figure 6b). These clones with suppressed level of ShcC showed the same morphological features of neurite formation in tissue culture condition as observed in the cells transfected with ShcC siRNAs (data not shown). The volumes and weights of subcutaneous tumors in nude mice were measured at 6 weeks after injections of the cells and evaluated in at least 4 independent injections per clone. Control LacZ miR RNAi clones (miLacZ-1, miLacZ-2) developed large tumor masses *in vivo* (Figure 6c), whereas remarkable reduction of the size and weight of tumors (or almost disappearance of tumors in some cases) was observed by the stable suppression of ShcC expression. These tumors from ShcC miR RNAi clones showed marked increase in numbers of apoptotic cells compared with control tissues as shown by terminal transferase dUTP nick-end labeling (TUNEL) staining. On the other hand, staining by a proliferation marker, Ki-67 showed no significant difference among each tumor tissue (Figure 6d).

Discussion

It has already been shown that some signal pathways strongly affect tumor progression and treatment resistance (Schwab *et al*., 2003). Other than the Trk family, the PI3K/Akt pathway (Opel *et al*., 2007), Ret (Iwamoto *et al*., 1993; Marshall *et al*., 1997), hepatocyte growth factor/c-Met pathway (Hecht *et al*., 2004) were reported to be closely associated with several diagnostic profiles and biological characteristics of neuroblastoma cells.

This is the first study to show that the expression of ShcC protein, a member of the Shc family docking proteins, is significantly correlated with malignant phenotypes associated with advanced neuroblastoma. Expression of both p52 and p67 isoforms of ShcC,

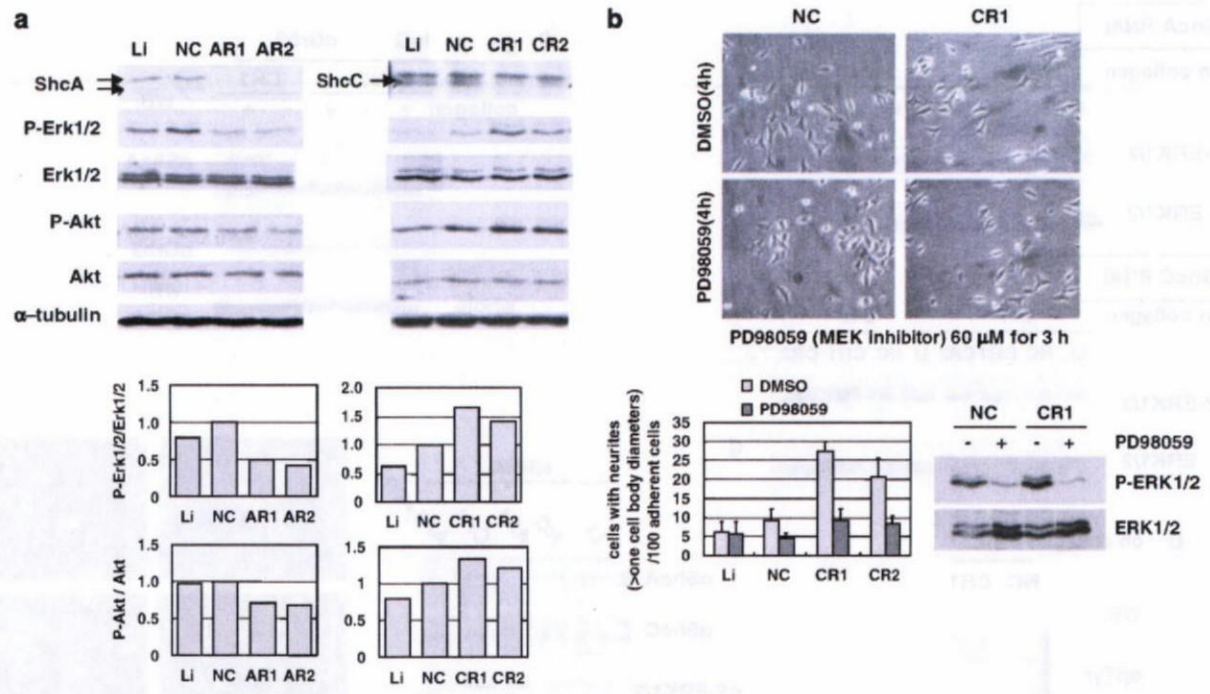

Figure 3 Persistent activation of extracellular signal-related kinase 1/2 (ERK1/2) in ShcC downregulation induces neurite outgrowth in TNB-1 cells. (**a**) Downregulation of ShcC positively affects the ERK1/2 and Akt pathway in TNB-1 cells. Activation of ERK1/2 and Akt in the cells treated with ShcA or ShcC siRNA were examined by western blotting. The levels of activation were quantified comparing to that of cells treated with control siRNA (NC). (**b**) Effect of MEK inhibitor on neurite outgrowth induced by ShcC RNAi in TNB-1 cells. The siRNA-transfected cells indicated were treated with dimethylsulphoxide (DMSO) or PD98059 and incubated for 3 h in the tissue culture condition, then counted for neurite-containing cells.

shows significant correlation with clinical stage and *MYCN* gene amplification whereas the expression of both isoforms of ShcA, p52 and p66, showed little association with those aspects. These results, in the protein level, give further evidence that ShcC is a factor which determines the prognosis of neuroblastoma, which was recently suggested by analysis of the mRNA expression of ShcC (Terui *et al*., 2005).

The biological analysis of TNB-1 cells treated with ShcC-specific siRNAs provided evidence that ShcC protein expressed in the neuroblastoma cells is suppressing the differentiation of neuroblastoma cells. Neurite outgrowth of TNB-1 cells, induced by downregulation of ShcC was dependent on sustained activation of the MEK/ERK pathway. Sustained activation of the ERK pathway triggered by factors such as NGF is required for neuronal differentiation in some neuronal tumor cells such as PC12 cells (Qui and Green, 1992; Yaka *et al*., 1998). The fact that constitutively activated Raf–ERK signaling induced neurite outgrowth in the same cell line (Supplementary Figure C), such as the RTK-related pathway might induce the ERK activation and cellular differentiation in TNB-1 cells, although NGF stimulation failed to induce neurite elongation of TNB-1 cells (data not shown).

Interestingly, elevation in the level of phosphorylated ShcA followed by activation of the ERK pathway by ShcA–Grb2 signals was observed in TNB1 when the ShcC protein expression was suppressed by RNAi. This activation of the ShcA–Grb2–ERK pathway caused by downregulation of ShcC may be due to a competitive effect between ShcC and ShcA for binding to certain RTKs. This possibility is supported by another experiment showing that both EGF-induced phosphorylation of ShcA and complex formation between ShcA and Grb2 in KU-YS cells are suppressed by the expression of ShcC in a dose-dependent manner. It was shown that the expression of the PTB domains of ShcC partially interfered with the binding of endogenous ShcA to activated EGFR in 293 cells (O'Bryan *et al*., 1998). These data are consistent with our current findings described above. It is suspected that some types of differentiation signals mediated by ShcA are blocked by the overexpression of ShcC in some neuroblastoma cells such as TNB-1, and the suppression of ShcC protein by RNAi causes the ShcA-mediated differentiation of these cells.

Elevated level of ShcA phosphorylation and ERK activation induced by ShcC downregulation was more significant under the stimulation of collagen I than without any ECM stimulation. In addition, in suspending condition we could not detect any activation of ShcA nor ERK signal after ShcC downregulation (Supplementary Figure E). These results indicate that the difference between ShcA and ShcC might be in interaction with matrix-adhesion signals. ShcA is considered to be implicated in the adherent related pathway, phosphorylated by forming a complex with

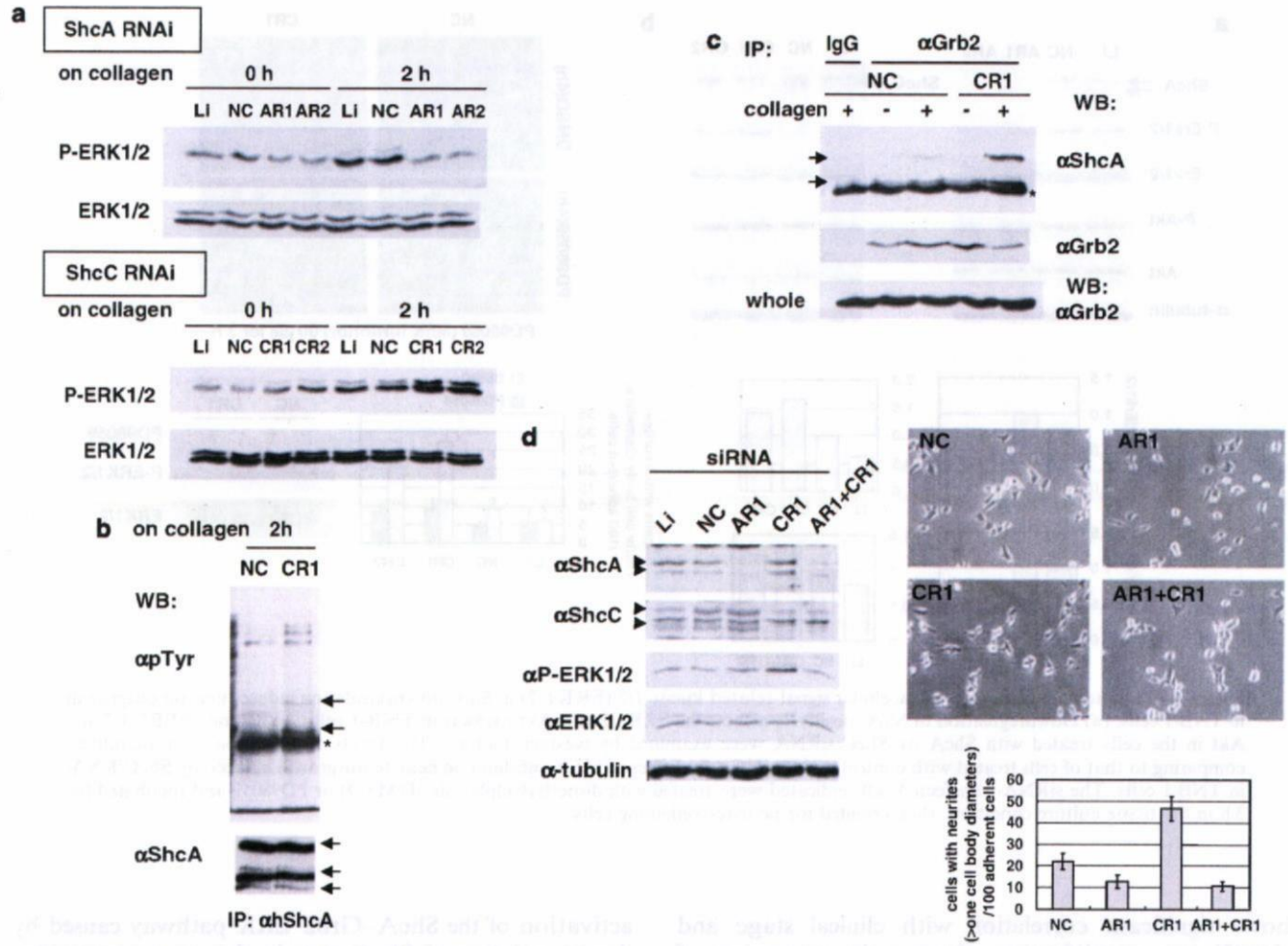

Figure 4 Elevation of extracellular signal-regulated kinase ()-activated level in ShcC-knockdown cells is increased by collagen stimulation by ShcA–Grb2 signaling. (**a**) Elevation of the ERK1/2-activated level due to ShcC downregulation is further increased 2 h after collagen stimulation. siRNAs of ShcA/ShcC-transfected TNB-1 cells (AR1, AR2/CR1, CR2, respectively) were incubated in the tissue culture condition for 70 h and stimulated by collagen type I. Duplicated cells were harvested 0 and 2 h after collagen stimulation (as described in 'Materials and methods'). (**b**) After collagen stimulation ShcA was phosphorylated more strongly in ShcC-knockdown cells than the control cells. Asterisks show heavy chains of immunoglobulin. (**c**) ShcA–Grb2 complex formation (upper panel) were increased by downregulation of ShcC. (**d**) The ShcA-knockdown effect on the neurite outgrowth in cells transfected with ShcC siRNA was evaluated by the same method performed in Figure 2Ba. The number of neurites observed in the cells transfected with both ShcA and ShcC siRNA was obviously decreased compared to cells transfected with only ShcC siRNA.

Fyn (Wary *et al*., 1998) through its proline-rich region that is not conserved in ShcC.

In tissue culture and in transgenic mice, signaling through Fyn has been closely associated with neurite extension and cell adhesion (Brouns *et al*., 2000, 2001). Berwanger *et al*. (2002) referred to the inverse correlation between the expression of Fyn and progression of neuroblastoma from 94 primary neuroblastoma specimens, showing that expressed Fyn-induced differentiation and growth arrest of neuroblastoma cell lines. Another report indicated that active Fyn kinase induces a lasting activation of the MAPK pathway through inhibition of MAPK phosphatase 1 (Wellbrock *et al*., 2002). We confirmed that neurite outgrowth of ShcC-knockdown TNB-1 cells was suppressed by Src family inhibitor, PP2 (Supplementary Figure H). These data suggest the possibility that Integrin–Fyn–ShcA signals could be closely associated with the differentiation of TNB-1 cells induced by ShcC downregulation along with the signals of RTK–ShcA/ShcC.

Noticeably, the interference of the ShcA-mediated signaling by ShcC protein is independent of tyrosine phosphorylation of ShcC. The function of the nonphosphorylated domain of ShcC such as SH2 might be also highlighted. As for the difference in the downstream signaling between ShcC and ShcA, little is known so far. Regarding to this point, Nakamura *et al*. (2002) indicated that inhibition of NGF-induced ERK activation by the expression of ShcC was due to the different Grb2-binding capacity between ShcA and ShcC in response to NGF. It was previously reported that ShcA preferentially binds to TrkA (Yamada *et al*., 2002), which is the key receptor against NGF due to neurite outgrowth with the sustained ERK phosphorylation,

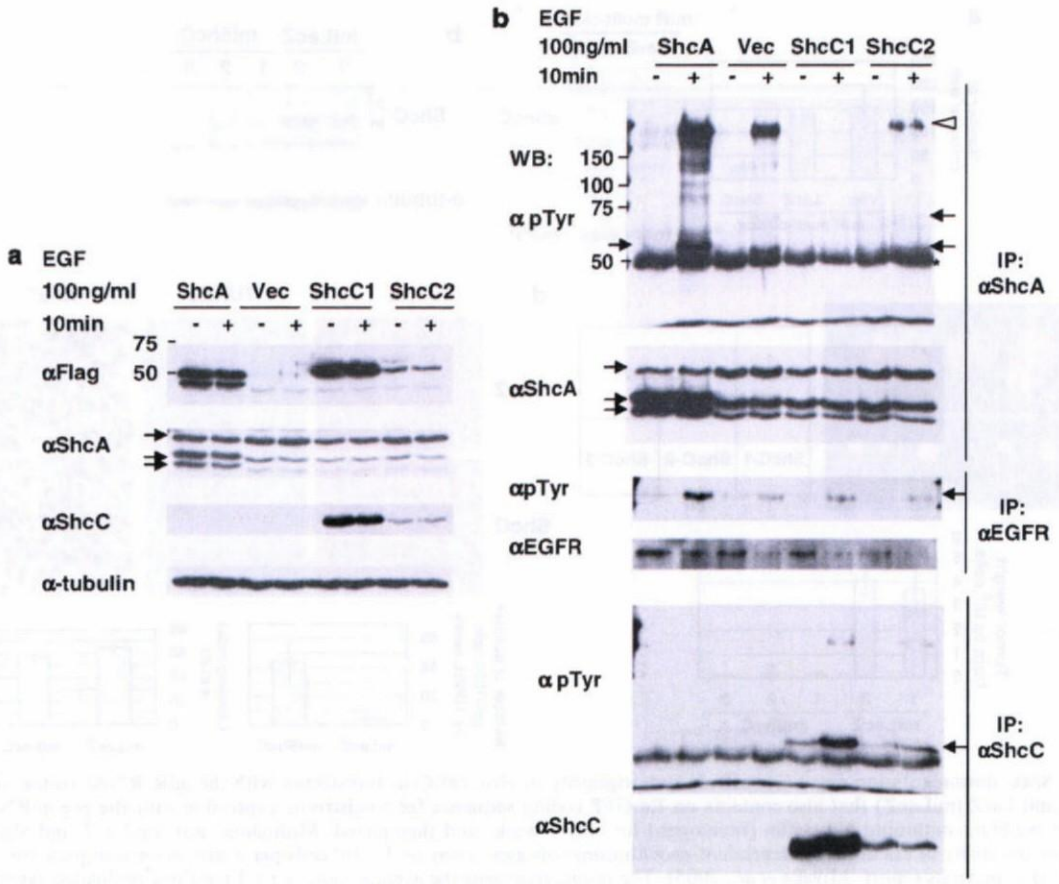

Figure 5 High expression of ShcC suppresses the phosphorylation of ShcA in KU-YS cells stimulated by epidermal growth factor (EGF). We generated stable clones of KU-YS cells expressing Flag-tagged ShcA and diverse levels of p52ShcC (ShcC1 and ShcC2) other than clones transfected with the control vector. (**a**) Each expression level was detected by western analysis. (**b**) Levels of expression and tyrosine phosphorylation of EGFR (middle panel), ShcA (upper panel) and ShcC (lower panel) were analysed by immunoprecipitation and immunoblotting using the antibodies indicated in figure in the KU-YS clone cells stimulated by EGF (as described in 'Materials and methods'). Asterisks show heavy chains of immunoglobulin.

whereas ShcC associated with TrkB rather than TrkA (O'Bryan *et al.*, 1998; Liu and Meakin, 2002). In neuroblastoma, the function of signal pathways downstream of these two neurotrophin receptors might be quite different (Nakagawara *et al.*, 1993), also suggesting the distinct function of downstream signal mediated by ShcC.

The effect of ShcC knockdown in *in vivo* tumorigenicity was quite remarkable comparing the effect in growth rate in tissue culture condition. We found that anchorage-independent growth in cells was also dramatically decreased by knockdown of ShcC as shown by soft agar assay (Figure 6a). Furthermore, the proportion of apoptotic cells in the nude mouse tumors generated from neuroblastoma cells *in vivo* was remarkably increased by the knockdown of ShcC. In recent study, Magrassi *et al.* (2005) showed that ShcC positively effects on cell survival by PI3K–AKT pathway in glioma cells using dominant negative form of ShcC. Theses data indicate that ShcC has additional function in the protection from some types of apoptosis in addition to the induction of differentiation of cells.

It was indicated that ShcC might have a potent function for tumor progression in neuroblastoma by suppressing the differentiation and by promoting the anchorage-independent growth in the majority of neuroblastoma cells which has high expression of ShcC protein. From these points of view, we suggest that ShcC is a potent tool for predicting the phenotype of neuroblastoma and is also a good candidate for therapeutic targets of advanced neuroblastoma.

Materials and methods

Cell culture and tissue samples

DLD-1 cells and all cell lines of neuroblastomas in this study were prepared as described in the previous report (Miyake *et al.*, 2002). These cells were cultured in an RPMI 1640 medium with 10% fetal calf serum (FCS) (Sigma, St Louis, MO, USA) at 37 °C in an atmosphere containing 5% CO_2.

Anonymous 46 frozen neuroblastoma tissues were used in this study. The samples were divided into three subsets using Brodeur's classification; type I (stage 1, 2 or 4S; a single copy of *MYCN*), type II (stage 3 or 4; a single copy of *MYCN*) and type III (all stages; amplification of *MYCN*) (Brodeur and Nakagawara, 1992; Ohira *et al.*, 2003). A total of 15 samples belonged to type I, 18 samples to type II and 13 samples to type III. Staging classification was according to the

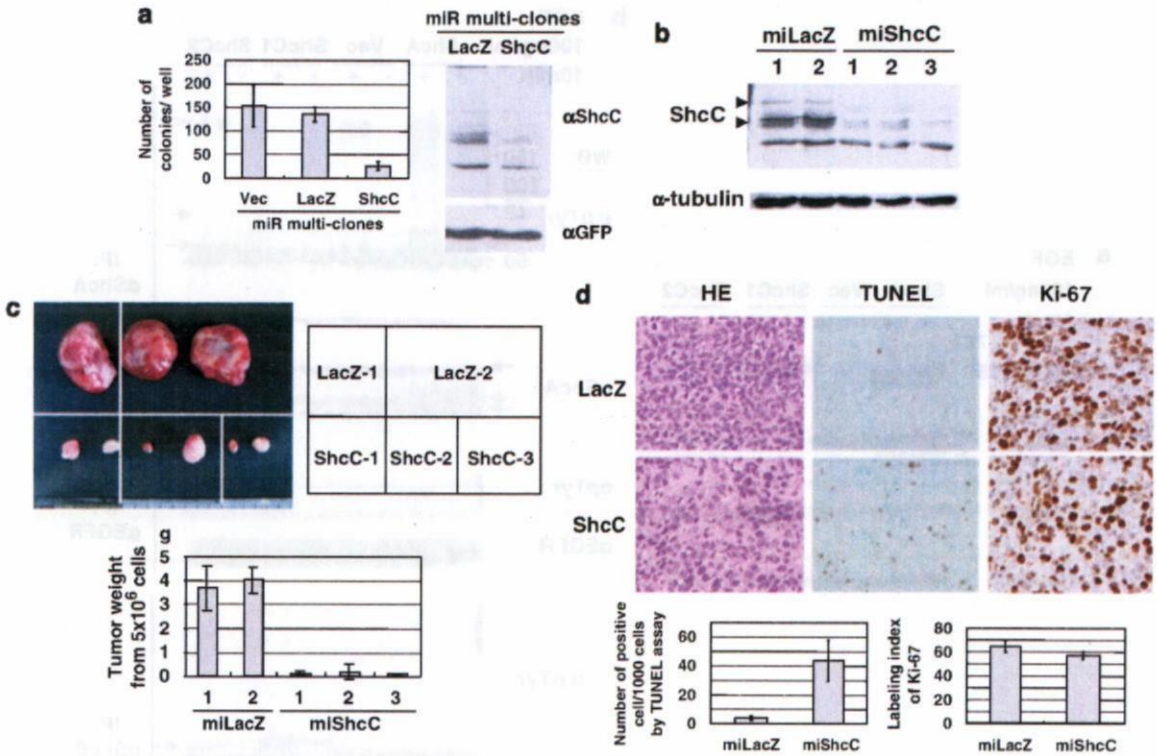

Figure 6 ShcC downregulation negatively affects tumorigenicity *in vivo*. (**a**) Cells transfected with the miR RNAi vector for ShcC (miShcC) and LacZ (miLacZ) that also contains an EmGFP coding sequence for co-cistronic expression with the pre-miRNA were cultured in medium containing blasticidin (Invivogen) for only 1 week, and then mixed. Multiclone cells for LacZ and ShcC were analysed for the ability of anchorage-independent growth using soft agar assay by 1×10^4 cells per a well of six-well plate for 3 weeks (as described in previous report: Miyake *et al*., 2005). The results represent the average value (± s.d.) of three replicated experiments. (**b**) Expression levels of ShcC in clones of TNB-1 cells stably transfected with miR RNAi expression vector for LacZ (miLacZ-1 and miLacZ-2) and ShcC (miShcC-1, -2 and -3) were detected by western analysis using αhShcC (as described in 'Materials and methods'). (**c**) Nude mouse tumors derived from two clones of LacZ miR RNAi and three clones of ShcC. Upper panel: Photographs of tumors from nude mice at 6 weeks after subcutaneous injections of 5×10^6 cloned cells (bar: 20 mm); lower panel: ability of *in vivo* tumorigenicity is shown by average weight (±) of four tumor derived from each clone. (**d**) ShcC-knockdown cells show tendency to apoptosis *in vivo*. Upper panel: Photographs of a cross-section of each tumor tissues from miLacZ-1 and miShcC-2 using microscope at a magnification of × 400, that were stained with hematoxylin and eosin (HE), diaminobenzidine (DAB) by terminal transferase dUTP nick-end labeling (TUNEL) assay and anti-Ki-67 antibody (bar: 25 μm); lower panel: the tendency to apoptosis was defined as the number of positive stained cells per 1000 tumor cells in TUNEL assay and the proliferating activity was indicated as the labeling index of Ki-67 by counting 1000 tumor cells. The data show the average scores ± s.d. of positive cells in three different areas of each slide. Staining of each sample was owing to the procedure by SRL Inc.

International Neuroblastoma Staging System and *N-Myc* amplification (> 10 copy) accepted as a poor prognostic risk factor was checked before clinical intervention.

Reagents

The polyclonal antibodies against the CH1 domain of human ShcC (amino acid 225–324):αhShcC were generated by the same method as described previously (Miyake *et al*., 2002). Polyclonal antibodies of human ShcA:αhShcA were prepared as described in previous reports (Miyake *et al*., 2002).

Other antibodies were purchased as follows: antiphosphotyrosine antibody (4G10) (Upstate Biotechnology Inc., Charlottesville, VA, USA), anti-ShcA/ShcC monoclonal antibodies: αShcA/αShcC (BD Transduction Laboratories, San Diego, CA, USA), anti-α-tubulin antibody (Zymed Laboratories, San Francisco, CA, USA), anti-p44/42 MAPK (ERK1/2), antiphospho-p44/42 MAPK (P-ERK1/2), anti-Akt, and antiphospho-Akt (Ser473) (P-Akt) antibodies (Cell Signaling, Danvers, MA, USA), anti-chromogranin A (ChrA) antibody (Santa Cruz Biotechnology, Santa Cruz, CA, USA), anti-GAP43 antibody (Zymed Laboratories), anti-MAP2 antibody (Santa Cruz Biotechnology), anti-c-Src antibody (Upstate Biotechnology Inc.), anti-phospho-Src family antibody (Tyr416) (Cell Signaling), anti-Grb2 antibody (BD Transduction Laboratories), anti-T7tag antibody (Novagen, San Diego, CA, USA) and anti-Flag M2 antibody (Sigma). As secondary antibodies, horseradish peroxidase-conjugated anti-rabbit and anti-mouse IgGs (GE Healthcare, Buckinghamshire, UK) were used. All inhibitors used in this study (PD98059, LY294002, PP2 and PP3) were purchased from Calbiochem, San Diego, CA, USA.

Cell stimulation, immunoprecipitation and immunoblotting

Cell stimulation analysis with EGF (Wako) was performed as described (Miyake *et al*., 2002). The cells were starved for 24 h and treated for 5 min with EGF (100 ng/ml). As for stimulation with collagen type I, cultured cells with or without serum for 24 h were detached from culture dishes by pipette treatment and after the suspending condition for 30 min, seeded onto a collagen type I-coated dish (Iwaki, Tokyo, Japan). Cells were harvested after 2 h using PLC lysis buffer. Control cells were harvested before the attachment on the collagen I-coated

surface. The immunoprecipitation and western analysis were performed using the procedure described in a previous report (Miyake *et al*., 2002).

Quantification and statistical analysis of expression levels of ShcC/ShcA

The intensity of each band obtained by western analysis was measured using a molecular imager (GS-800; Bio-Rad, Hercules, CA, USA) and standardized according to control signals, such as the bands of TNB-1 and α-tubulin.

t-Test performed by Excel was used to evaluate the significance of the two groups quantified expression levels of indicated molecules.

Knockdown of ShcA/ShcC by RNA interference

For siRNAs, Stealth RNA duplex oligoribonucleotides (Invitrogen, Carlsbad, CA, USA) was used to knockdown ShcC/ShcA protein. The following two 25-mer oligonucleotide pairs for each molecule were available. As for ShcC, CR1: 5′-GCUGGCCAAAGCGCUCUAUGACAAU-3′ (nucleotides 141–165), CR2: 5′-CCAAGAUCUUUGUGGCGCACA GCAA-3′ (nucleotides 2447–2471). As negative controls for each oligonucleotide pair, cc1: GGCUCCAGAACGGCCUUAGU AACAU-3′, cc2: GGAAACCGACAACUACGAUGUCAAU, respectively. As for ShcA, AR1: 5′-GGAGUAACCUGAA AUUUGCUGGAAU-3′ (nucleotides 335–359). AR2: 5′-GCCU UCGAGUUGCGCUUCAAACAAU-3′ (nucleotides 689–611). As a negative control for each, ac1: GGAAACCGUAAUAUU CGGUGUGAA, ac2: 5′-UGCCGCGAUUCGCGUUACAAC UUAAU, respectively. As the other negative control for universal siRNA, Stealth RNAi Negative Control Duplexes (Medium GC Duplex) (Invitrogen) was used (NC). Cells were transfected with siRNA using Lipofectamine 2000 (Invitrogen) according to the manufacturer's instructions. Cells (5×10^5 per well of a six-well plate) in suspending condition were transfected twice at 24 h interval (5 μl of 20 μM siRNA each) and analysed 48 h after second transfection.

A system stably expressing miRNA was generated using the BLOCK-iT Pol II miR RNAi Expression Vector Kit with EmGFP (Invitrogen) according to the manufacturer's instructions. In the generation of the miR RNAi vector for humans, ShcC was chosen as the target sequence, using the top/bottom oligo sequence: 5′-TGCTGCTTGGAGGCTTTCTCTTCTT GGTTTTGGCCACTGACTGACCAAGAAGAAAGCCTC CAAG-3′/5′-CCTGCTTGGAGGCTTTCTTCTTGGTCAGTC AGTGGCCAAAACCAAGAAGAGAAAGCCTCCAAGC-3′. Cells stably expressing the miR RNAi vector for ShcC (miShcC) and LacZ (miLacZ), that were also expressing green fluorescent protein were established and cultured in medium containing blasticidin (InvivoGen, San Diego, CA, USA) at a concentration of 15 μg/ml for 3 weeks. Three clones expressing the ShcC RNAi vector were selected by significant suppression of the ShcC protein (< 10%), and two clones from the control LacZ vector were also selected. Cells transfected with miR-negative control plasmid (one of kit components) were used as other control cells (Vec).

Generation of KU-YS cells stably expressing ShcA/ShcC

The full-length human ShcA cDNA for transfection was donated by Dr N Goto. ShcA and ShcC cDNAs were inserted with C-terminal Flag epitope tag into a mammalian expression vector pcDNA3.1A. All parts amplified by PCR were verified by sequencing. The stable expression of the full-length of ShcA and full-length of ShcC in KU-YS cells were obtained by transfection using transfection reagent Lipofectamine 2000 (Invitrogen) according to the manufacturer's instructions. The KU-YS cells transfected with pcDNA3.1 vector (mock) were used as a control. Then, cells were selected according to the method described previously and the expression level of each independent clone was evaluated by immunoblotting analysis.

Acknowledgements

This work was supported by a Grant-in-Aid from the Ministry of Health, Labor and Welfare of Japan for the third-term Comprehensive 10-year Strategy for Cancer Control.

References

Berwanger B, Hartmann O, Bergmann E, Bernard S, Nielsen D, Krause M *et al*. (2002). Loss of a FYN-regulated differentiation and growth arrest pathway in advanced stage neuroblastoma. *Cancer Cell* **2**: 377–386.

Brodeur GM, Nakagawara A. (1992). Molecular basis of clinical heterogeneity in neuroblastoma. *Am J Pediatr Hematol Oncol* **14**: 111–116.

Brouns MR, Matheson SF, Hu KQ, Delalle I, Caviness VS, Silver J *et al*. (2000). The adhesion signaling molecule p190 RhoGAP is required for morphogenetic processes in neural development. *Development* **127**: 4891–4903.

Brouns MR, Matheson SF, Settleman J. (2001). p190 RhoGAP is the principal Src substrate in brain and regulates axon outgrowth, guidance and fasciculation. *Nat Cell Biol* **3**: 361–367.

Dhillon AS, Meikle S, Peyssonnaux C, Grindlay J, Kaiser C, Steen H *et al*. (2003). A Raf-1 mutant that dissociates MEK/extracellular signal-regulated kinase activation from malignant transformation and differentiation but not proliferation. *Mol Cell Biol* **23**: 1983–1993.

Giudici AM, Sher E, Pelagi M, Clementi F, Zanini A. (1992). Immunolocalization of secretogranin II, chromogranin A, and chromogranin B in differentiating human neuroblastoma cells. *Eur J Cell Biol* **58**: 383–389.

Hecht M, Papoutsi M, Tran HD, Wilting J, Schweigerer L. (2004). Hepatocyte growth factor/c-Met signaling promotes the progression of experimental human neuroblastomas. *Cancer Res* **64**: 6109–6118.

Hecker TP, Grammer JR, Gillespie GY, Stewart Jr J, Gladson CL. (2002). Focal adhesion kinase enhances signaling through the Shc/extracellular signal-regulated kinase pathway in anaplastic astrocytoma tumor biopsy samples. *Cancer Res* **62**: 2699–2707.

Hinsby AM, Lundfald L, Ditlevsen DK, Korshunova I, Juhl L, Meakin SO *et al*. (2004). ShcA regulates neurite outgrowth stimulated by neural cell adhesion molecule but not by fibroblast growth factor 2: evidence for a distinct fibroblast growth factor receptor response to neural cell adhesion molecule activation. *J Neurochem* **91**: 694–703.

Iwamoto T, Taniguchi M, Wajjwalku W, Nakashima I, Takahashi M. (1993). Neuroblastoma in a transgenic mouse carrying a metallothionein/ret fusion gene. *Br J Cancer* **67**: 504–507.

Leevers SJ, Paterson HF, Marshall CJ. (1994). Requirement for Ras in Raf activation is overcome by targeting Raf to the plasma membrane. *Nature* **369**: 411–414.

Liu HY, Meakin SO. (2002). ShcB and ShcC activation by the Trk family of receptor tyrosine kinases. *J Biol Chem* **277**: 26046–26056.

Magrassi L, Conti L, Lanterna A, Zuccato C, Marchionni M, Cassini P *et al*. (2005). Shc3 affects human high-grade astrocytomas survival. *Oncogene* **24**: 5198–5206.

Marshall GM, Peaston AE, Hocker JE, Smith SA, Hansford LM, Tobias V *et al*. (1997). Expression of multiple endocrine neoplasia 2B RET in neuroblastoma cells alters cell adhesion *in vitro*, enhances

metastatic behavior *in vivo*, and activates Jun kinase. *Cancer Res* **57**: 5399–5405.

Miyake I, Hakomori Y, Misu Y, Nakadate H, Matsuura N, Sakamoto M *et al.* (2005). Domain-specific function of ShcC docking protein in neuroblastoma cells. *Oncogene* **24**: 3206–3215.

Miyake I, Hakomori Y, Shinohara A, Gamou T, Saito M, Iwamatsu A *et al.* (2002). Activation of anaplastic lymphoma kinase is responsible for hyperphosphorylation of ShcC in neuroblastoma cell lines. *Oncogene* **21**: 5823–5834.

Moro L, Venturino M, Bozzo C, Silengo L, Altruda F, Beguinot L *et al.* (1998). Integrins induce activation of EGF receptor: role in MAP kinase induction and adhesion-dependent cell survival. *EMBO J* **17**: 6622–6632.

Nakagawara A, Arima-Nakagawara M, Scavarda NJ, Azar CG, Cantor AB, Brodeur GM. (1993). Association between high levels of expression of the TRK gene and favorable outcome in human neuroblastoma. *N Engl J Med* **328**: 847–854.

Nakagawara A, Brodeur GM. (1997). Role of neurotrophins and their receptors in human neuroblastomas: a primary culture study. *Eur J Cancer* **33**: 2050–2053.

Nakamura T, Komiya M, Gotoh N, Koizumi S, Shibuya M, Mori N. (2002). Discrimination between phosphotyrosine-mediated signaling properties of conventional and neuronal Shc adapter molecules. *Oncogene* **21**: 22–31.

Nakamura T, Muraoka S, Sanokawa R, Mori N. (1998). N-Shc and Sck, two neuronally expressed Shc adapter homologs. Their differential regional expression in the brain and roles in neurotrophin and Src signaling. *J Biol Chem* **273**: 6960–6967.

Nakamura T, Sanokawa R, Sasaki Y, Ayusawa D, Oishi M, Mori N. (1996). N-Shc: a neural-specific adapter molecule that mediates signaling from neurotrophin/Trk to Ras/MAPK pathway. *Oncogene* **13**: 1111–1121.

O'Bryan JP, Lambert QT, Der CJ. (1998). The src homology 2 and phosphotyrosine binding domains of the ShcC adaptor protein function as inhibitors of mitogenic signaling by the epidermal growth factor receptor. *J Biol Chem* **273**: 20431–20437.

O'Bryan JP, Songyang Z, Cantley L, Der CJ, Pawson T. (1996). A mammalian adaptor protein with conserved Src homology 2 and phosphotyrosine-binding domains is related to Shc and is specifically expressed in the brain. *Proc Natl Acad Sci USA* **93**: 2729–2734.

Ohira M, Morohashi A, Inuzuka H, Shishikura T, Kawamoto T, Kageyama H *et al.* (2003). Expression profiling and characterization of 4200 genes cloned from primary neuroblastomas: identification of 305 genes differentially expressed between favorable and unfavorable subsets. *Oncogene* **22**: 5525–5536.

Opel D, Poremba C, Simon T, Debatin KM, Fulda S. (2007). Activation of Akt predicts poor outcome in neuroblastoma. *Cancer Res* **67**: 735–745.

Osajima-Hakomori Y, Miyake I, Ohira M, Nakagawara A, Nakagawa A, Sakai R. (2005). Biological role of anaplastic lymphoma kinase in neuroblastoma. *Am J Pathol* **167**: 213–222.

Pelicci G, Dente L, De Giuseppe A, Verducci-Galletti B, Giuli S, Mele S *et al.* (1996). A family of Shc related proteins with conserved PTB, CH1 and SH2 regions. *Oncogene* **13**: 633–641.

Qui MS, Green SH. (1992). PC12 cell neuronal differentiation is associated with prolonged p21ras activity and consequent prolonged ERK activity. *Neuron* **9**: 705–717.

Ravichandran KS. (2001). Signaling via Shc family adapter proteins. *Oncogene* **20**: 6322–6330.

Sakai R, Henderson JT, O'Bryan JP, Elia AJ, Saxton TM, Pawson T. (2000). The mammalian ShcB and ShcC phosphotyrosine docking proteins function in the maturation of sensory and sympathetic neurons. *Neuron* **28**: 819–833.

Schwab M, Westermann F, Hero B, Berthold F. (2003). Neuroblastoma: biology and molecular and chromosomal pathology. *Lancet Oncol* **4**: 472–480.

Stokoe D, Macdonald SG, Cadwallader K, Symons M, Hancock JF. (1994). Activation of Raf as a result of recruitment to the plasma membrane. *Science* **264**: 1463–1467.

Terui E, Matsunaga T, Yoshida H, Kouchi K, Kuroda H, Hishiki T *et al.* (2005). Shc family expression in neuroblastoma: high expression of shcC is associated with a poor prognosis in advanced neuroblastoma. *Clin Cancer Res* **11**: 3280–3287.

Wary KK, Mainiero F, Isakoff SJ, Marcantonio EE, Giancotti FG. (1996). The adaptor protein Shc couples a class of integrins to the control of cell cycle progression. *Cell* **87**: 733–743.

Wary KK, Mariotti A, Zurzolo C, Giancotti FG. (1998). A requirement for caveolin-1 and associated kinase Fyn in integrin signaling and anchorage-dependent cell growth. *Cell* **94**: 625–634.

Wellbrock C, Weisser C, Geissinger E, Troppmair J, Schartl M. (2002). Activation of p59(Fyn) leads to melanocyte dedifferentiation by influencing MKP-1-regulated mitogen-activated protein kinase signaling. *J Biol Chem* **277**: 6443–6454.

Yaka R, Gamliel A, Gurwitz D, Stein R. (1998). NGF induces transient but not sustained activation of ERK in PC12 mutant cells incapable of differentiating. *J Cell Biochem* **70**: 425–432.

Yamada M, Numakawa T, Koshimizu H, Tanabe K, Wada K, Koizumi S *et al.* (2002). Distinct usages of phospholipase C gamma and Shc in intracellular signaling stimulated by neurotrophins. *Brain Res* **955**: 183–190.

Supplementary Information accompanies the paper on the Oncogene website (http://www.nature.com/onc)

Int. J. Cancer: **123**, 2087–2094 (2008)

Expression of *TSLC1*, a candidate tumor suppressor gene mapped to chromosome 11q23, is downregulated in unfavorable neuroblastoma without promoter hypermethylation

Kiyohiro Ando[1], Miki Ohira[1], Toshinori Ozaki[1], Atsuko Nakagawa[2], Kohei Akazawa[3], Yusuke Suenaga[1], Yohko Nakamura[1], Tadayuki Koda[4], Takehiko Kamijo[1], Yoshinori Murakami[5] and Akira Nakagawara[1]*

[1]*Division of Biochemistry, Chiba Cancer Center Research Institute, Chiba, Japan*
[2]*Division of Clinical Laboratory, National Center for Child Health and Development, Tokyo, Japan*
[3]*Division of Medical Information, Niigata University Medical and Dental Hospital, Niigata, Japan*
[4]*Center for Functional Genomics, Hisamitsu Pharmaceutical Co. Inc., Chiba, Japan*
[5]*Division of Molecular Pathology, Department of Cancer Biology, Institute of Medical Science, The University of Tokyo, Tokyo, Japan*

Although it has been well documented that loss of human chromosome 11q is frequently observed in primary neuroblastomas, the smallest region of overlap (SRO) has not yet been precisely identified. Previously, we performed array-comparative genomic hybridization (array-CGH) analysis for 236 primary neuroblastomas to search for genomic aberrations with high-resolution. In our study, we have identified the SRO of deletion (10-Mb or less) at 11q23. Within this region, there exists a *TSLC1/IGSF4/CADM1* gene (*Tumor suppressor in lung cancer 1/Immunoglobulin superfamily 4/Cell adhesion molecule 1*), which has been identified as a putative tumor suppressor gene for lung and some other cancers. Consistent with previous observations, we have found that 35% of primary neuroblastomas harbor loss of heterozygosity (LOH) on *TSLC1* locus. In contrast to other cancers, we could not detect the hypermethylation in its promoter region in primary neuroblastomas as well as neuroblastoma-derived cell lines. The clinicopathological analysis demonstrated that *TSLC1* expression levels significantly correlate with stage, Shimada's pathological classification, *MYCN* amplification status, *TrkA* expression levels and DNA index in primary neuroblastomas. The immunohistochemical analysis showed that TSLC1 is remarkably reduced in unfavorable neuroblastomas. Furthermore, decreased expression levels of *TSLC1* were significantly associated with a poor prognosis in 108 patients with neuroblastoma. Additionally, TSLC1 reduced cell proliferation in human neuroblastoma SH-SY5Y cells. Collectively, our present findings suggest that *TSLC1* acts as a candidate tumor suppressor gene for neuroblastoma.

Key words: *TSLC1/IGSF4/CADM1*; neuroblastoma; 11q23; tumor suppressor

Neuroblastoma is one of the most common solid tumors in childhood and originates from the sympathoadrenal lineage of neural crest. Its biological as well as clinical behavior is highly heterogeneous in different prognostic subsets. Tumors found in patients under 1 year of age often regress spontaneously or differentiate and result in a favorable prognosis.[1] In a sharp contrast to these favorable neuroblastomas, tumors found in patients over 1 year of age are often aggressive with an unfavorable prognosis despite an intensive therapy. A large number of multiple genomic aberrations including DNA index, *MYCN* amplification status, allelic loss of the distal part of chromosome 1p and the gain of chromosome 17q have been identified in neuroblastoma.[2,3]

Alternatively, allelic loss of 11q has been frequently observed in advanced stage of neuroblastoma with single copy of *MYCN*. Indeed, 30% of tumors harbor allelic loss of 11q, and it might be an independent prognostic indicator for clinically high-risk patients without *MYCN* amplification.[4,5] Aberrant deletions of 11q often occur in a distal part of its long arm. Although several lines of evidence delineated the smallest region of overlaps (SRO) of deletions at 11q, it remains unclear whether there could exist a candidate tumor suppressor gene(s) implicated in biological and clinical behaviors of neuroblastoma.[6,7] Recently, we have performed an array-comparative genomic hybridization (array-CGH) analysis using 236 primary neuroblastomas and finally defined the SRO (10-Mb or less) at 11q23.[3,8] During our extensive search for the already identified candidate tumor suppressor gene(s) within this region, we have found that *TSLC1/IGSF4/CADM1* gene is localized within this region.

TSLC1 gene has been originally identified as a putative tumor suppressor for non-small-cell lung cancer (NSCLC) located at chromosome 11q23 by functional complementation strategy of a human lung cancer cell line. The downregulation of *TSLC1* gene was frequently detected in various human cancers including NSCLC, prostate cancers, hepatocellular carcinomas and pancreatic cancers through its allelic loss as well as hypermethylation of its promoter region. In spite of an extensive mutation search, only 2 inactivating *TSLC1* gene mutations were detected in 161 primary tumors and tumor-derived cell lines, suggesting that *TSLC1* is rarely mutated in human cancers.[9] *TSLC1* encodes a single membrane-spanning glycoprotein involved in cell–cell adhesion through homophilic trans interaction.[10] Accumulating evidence indicates that TSLC1 is significantly associated with biological aggressiveness and metastasis of certain types of cancer,[11–16] whereas the functional significance of TSLC1 in neuroblastoma remains elusive.

In the present study, we have further delineated the SRO of 11q deletion in primary neuroblastoma by array-CGH analysis and finally identified *TSLC1* gene within this region. In contrast to the other cancers, hypermethylation of *TSLC1* promoter region was undetectable in neuroblastoma. Intriguingly, the expression levels of *TSLC1* gene were highly associated with clinical stage, Shimada's pathological classification, *MYCN* amplification status, *TrkA* expression levels and DNA index in primary neuroblastoma.

Additional Supporting Information may be found in the online version of this article.

Abbreviations: array-CGH, array-comparative genomic hybridization; BAC, bacterial artificial chromosome; LOH, loss of heterozygosity; PARP, poly(ADP-ribose) polymerase; SRO, smallest region of overlap; STS, sequence-tagged-site; TSA, trichostatin A; TSLC1, tumor suppressor in lung cancer 1.

Grant sponsors: Ministry of Health, Labour and Welfare for Third Term Comprehensive Control Research for Cancer; Ministry of Education, Culture, Sports, Science and Technology, Japan; Scientific Research from Japan Society for the Promotion of Science.

***Correspondence to:** Chiba Cancer Center Research Institute, 666-2 Nitona, Chuo-ku, Chiba 260-8717. Fax: +81-43-265-4459.
E-mail: akiranak@chiba-cc.jp

Received 21 February 2008; Accepted after revision 19 May 2008
DOI 10.1002/ijc.23776
Published online 22 August 2008 in Wiley InterScience (www.interscience.wiley.com).

Material and methods

Patients, tumor specimens and cell lines

One hundred and eight tumor specimens used in the present study were kindly provided from various institutions and hospitals in Japan (see Supplementary Information). Informed consent was obtained at each institution or hospital. All tumors were diagnosed clinically as well as pathologically as neuroblastoma and staged according to the International Neuroblastoma Staging System (INSS) criteria.[17] Twenty-seven patients were Stage 1, 15 Stage 2, 36 Stage 3, 23 Stage 4 and 7 Stage 4S. The patients were treated by the standard protocols as described previously.[18,19] *MYCN* copy number, *TrkA* mRNA expression levels and DNA index were measured as reported previously.[20] Our present study was approved by the Institutional Review Board of the Chiba Cancer Center (CCC7817).

Human tumor-derived cell lines were cultured in RPMI 1640 medium (Nissui, Tokyo, Japan) supplemented with 10% heat-inactivated fetal bovine serum (FBS, Invitrogen, Carlsbad, CA) and 50 μg/ml penicillin/streptomycin (Invitrogen) in an incubator with humidified air at 37°C with 5% CO_2.

Array-comparative genomic hybridization

Array-CGH analysis was performed using UCSF BAC array (2464 BACs, ≈1 Mb resolution) with 236 primary neuroblastomas. Detailed experimental procedures and the criteria for losses and gains were described previously.[3,20–22]

LOH analysis

Genomic DNA prepared from neuroblastomas and bloods was amplified by PCR-based strategy using the primer set, one of which was labeled with fluorescent dye CY5. The amplified fragments including 3 polymorphic STS markers encompassing *TSLC1*, *D11S4111*, *D11S2077* and *D11S1885*, were separated by 6% polyacrylamide gels containing 6 M urea using an automated ALF express DNA sequencer.

Semiquantitative and quantitative reverse transcription-PCR analysis

Total RNA was prepared from the indicated primary neuroblastomas, various human normal tissues and tumor-derived cell lines were subjected to semiquantitative RT-PCR using SuperScript II reverse transcriptase and random primers (Invitrogen), according to the manufacturer's instructions. Oligonucleotide primer set used to amplify *TSLC1* by semiquantitative RT-PCR was as follows: 5′-CATTTTGGAATTTGCCTGCT-3′ (sense) and 5′-GGCAGCAG-CAAAGAG TTTTC-3′ (antisense). Quantitative real-time PCR was carried out using TaqMan(R) Gene Expression Assay System (Applied Biosystems, Foster City, CA) as described previously.[20] In brief, expression levels were calculated as a ratio of mRNA level for a given gene relative to mRNA for *GAPDH* in the same cDNA. The oligonucleotide primers and TaqMan probes, labeled at the 5′-end with the reporter dye 6-carboxyfluorescein (FAM) and at the 3′-end with 6-carboxytetramethylrhodamine (TAMRA), were provided by Applied Biosystems (Hs00942508_m1).

Immunohistochemistry

A 4-μm-thick section of formalin-fixed, paraffin-embedded tissues were stained with hematoxylin and eosin and the adjacent sections were immunostained for TSLC1 using polyclonal anti-TSLC1 antibody (CC2) as described previously.[10] The BenchMark XT immunostainer (Ventana Medical Systems, Tucson, AZ) and 3-3′ diaminobenzidine detection kit (Ventana Medical Systems) were used to visualize TSLC1. Appropriate positive and negative control experiments were also performed in parallel for each immunostaining.

Small interfering RNA

TSLC1 siRNA (GUCAAUAAGAGUGACGACUUU) and Stealth RNAi Negative Control Duplex were purchased from Sigma-Aldrich (St. Louis, MO) and Invitrogen, respectively.

Transfection

Neuroblastoma-derived SH-SY5Y cells were transfected with the indicated combinations of expression plasmids or with siRNA against TSLC1 using LipofectAMINE 2000 or LipofectAMINE RNAiMAX transfection reagent (Invitrogen), according to the manufacturer's recommendations.

Colony formation assay

SH-SY5Y and SK-N-AS cells (1×10^5 cells/plate) were seeded in 6-well cell culture plates and transfected with or without the increasing amounts of the expression plasmid for TSLC1 (0, 250, 750 or 1,000 ng). Total amounts of plasmid DNA per transfection were kept constant (1 μg) with the empty plasmid (pcDNA3.1-Hygro (+); Invitrogen). Forty-eight hours after transfection, cells were transferred into the fresh medium containing hygromycin (at a final concentration of 200 μg/ml) and maintained for 14 days. Drug-resistant colonies were then stained with Giemsa's solution and numbers of drug-resistant colonies were scored.

Cell growth assay

SH-SY5Y cells (6×10^5 cells/dish) were seeded in 10-cm diameter cell culture dish and transiently transfected with siRNA against TSLC1 (240 pmol). Thirty-six hours after transfection, 2×10^4 cells were transferred into 6-well plates and transfected with 60 pmol of siRNA against TSLC1. At the indicated time points after transfection, number of viable cells was measured using a Coulter Counter (Coulter Electronics, Hialeah, Finland).

Bisulfite-sequencing

Sodium bisulfite-mediated modification of genomic DNA was performed using BisulFast Methylated DNA Detection Kit (Toyobo, Osaka, Japan), according to the manufacture's instructions. Modified genomic DNA was subjected to PCR-based amplification with a primer set as described previously.[23] The PCR products containing the promoter region of *TSLC1* gene were purified by PCR Purification Kit (Qiagen, Valencia, CA) and their nucleotide sequences were determined by using a 3730 DNA Analyzer (Applied Biosystem).

Statistical analysis

Fisher's exact tests were employed to examine possible associations between *TSLC1* expression and other prognostic indicators such as age. The difference between high and low expression levels of *TSLC1* was based on the mean value obtained from quantitative real-time PCR analysis. Kaplan-Meier survival curves were calculated, and survival distributions were compared using the log-rank test. Cox regression models were used to investigate the associations between *TSLC1* expression levels, age, *MYCN* amplification status, INSS and survival. Differences were considered significant if the p-value was less than 0.05.

Results

Array-comparative genomic hybridization analysis identifies the smallest region of overlaps of deletion in neuroblastoma at 11q23

We have previously performed array-CGH analysis using UCSF BAC array (2464 BACs, ≈1-Mb resolution) and 236 primary neuroblastomas.[3] In our array-CGH study, 66 tumors were revealed to have partial deletion of 11q as shown in Figure 1*a*, whose SRO were approximately 10-Mb long at 11q23 (from physical location of 110,979 to 119,806 kb in UCSC database, May 2006). To date, the data base analysis demonstrated that there could exist approximately 100 genes within this region. Of inter-

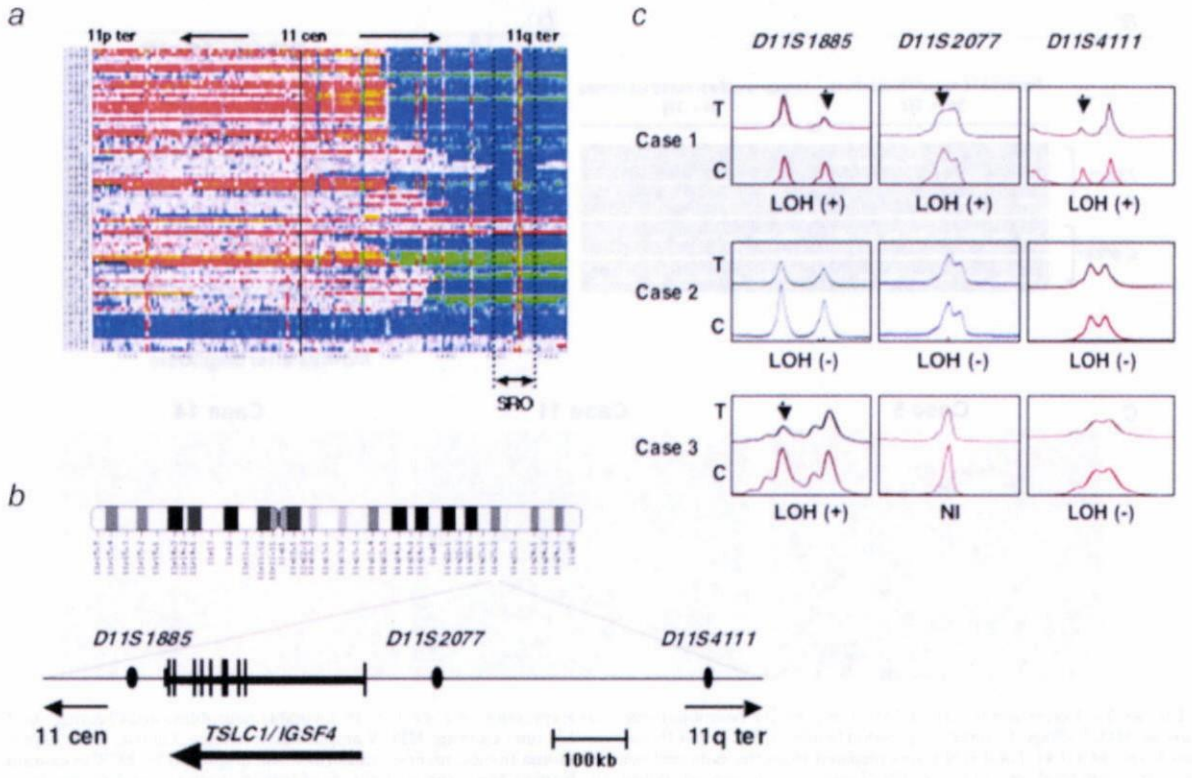

FIGURE 1 – Identification of the SRO of deletion at 11q in primary neuroblastoma. (*a*) Array-CGH analysis. Blue color indicates the position of the deleted area in each case. The smallest region of overlaps (SRO) of deletion at 11q is also shown. (*b*) The schematic drawing of the relative positions of 3 independent polymorphic markers at 11q23 used in the present study and *TSLC1* gene on human chromosome 11. (*c*) Representative electropherograms obtained from LOH analysis. Genomic DNA prepared from primary tumors (T) and their corresponding blood (C) was subjected to LOH analysis. Allelic losses are indicated by arrowheads. NI, not informative.

est, *TSLC1* gene which has been considered as a putative tumor suppressor for human lung as well as other cancers[9] locates within this region (Fig. 1*b*). These observations prompted us to perform loss of heterozygosity (LOH) as well as expression studies of *TSLC1* gene in primary neuroblastoma.

LOH at the TSLC1 locus is frequently detected in primary neuroblastoma

According to the previous observations,[9,24] tumor-specific downregulation of *TSLC1* gene might be largely attributed to loss of one allele in association with the hypermethylation of its promoter region in the remaining allele. To address whether LOH of *TSLC1* locus could be frequently detectable in primary neuroblastoma, we carried out LOH analysis using 3 independent fluorescently labeled polymorphic microsatellite markers (*D11S1885*, *D11S2077* and *D11S4111*) surrounding *TSLC1* gene (Fig. 1*b*). In accordance with the previous results,[9,25,26] the incidence of 11q23 LOH was 22% (7 of 32) and 45% (18 of 40) in favorable neuroblastomas (Stage 1 or 2) and unfavorable ones (Stage 3 or 4), respectively (data not shown). Statistical Fisher's exact test analysis revealed that the presence of LOH at this locus is associated with unfavorable neuroblastomas ($p = 0.0493$; data not shown). It is worth noting that LOH is detectable at *D11S1885* but not at *D11S4111* in Case 3 tumor (Fig. 1*c*), indicating that a putative chromosome breakpoint might exist between these loci.

Downregulation of TSLC1 expression is frequently observed in unfavorable neuroblastomas

Based on the previous observations,[11–16] the expression levels of *TSLC1* were significantly reduced in advanced stages of tumors as compared with those in early stages of tumors. We then examined the expression levels of *TSLC1* in 16 favorable neuroblastomas without *MYCN* amplification and 16 unfavorable ones with *MYCN* amplification. As clearly shown in Figure 2*a*, *TSLC1* was expressed at lower levels in unfavorable neuroblastomas relative to favorable ones as examined by semiquantitative RT-PCR. To ask whether there could exist a possible relationship between downregulation of *TSLC1* and *MYCN* amplification, we examined the expression levels of *TSLC1* in various neuroblastoma-derived cell lines bearing single copy of *MYCN* or *MYCN* amplification. As shown in Supplementary Figure 1*a*, a significant downregulation of *TSLC1* expression was detected in 2 of 6 neuroblastoma cell lines carrying single copy of *MYCN* (OAN and CNB-RT) and in 4 of 21 (CHP134, KP-N-NS, SK-N-DZ and NMB) bearing *MYCN* amplification as examined by semiquantitative RT-PCR. In addition, there was no obvious correlation between the expression levels of *TSLC1* and loss of 11q except OAN, SK-N-DZ and NMB. Next, we checked the expression levels of *TSLC1* in various human adult and fetal tissues. As seen in Supplementary Figure 1*b*, *TSLC1* was highly expressed in normal neuronal tissues, adrenal gland, testis, prostate and liver. Our present results suggest that *TSLC1* is expressed in normal neuronal tissues and its expression levels might be regulated in a *MYCN*-dependent manner in

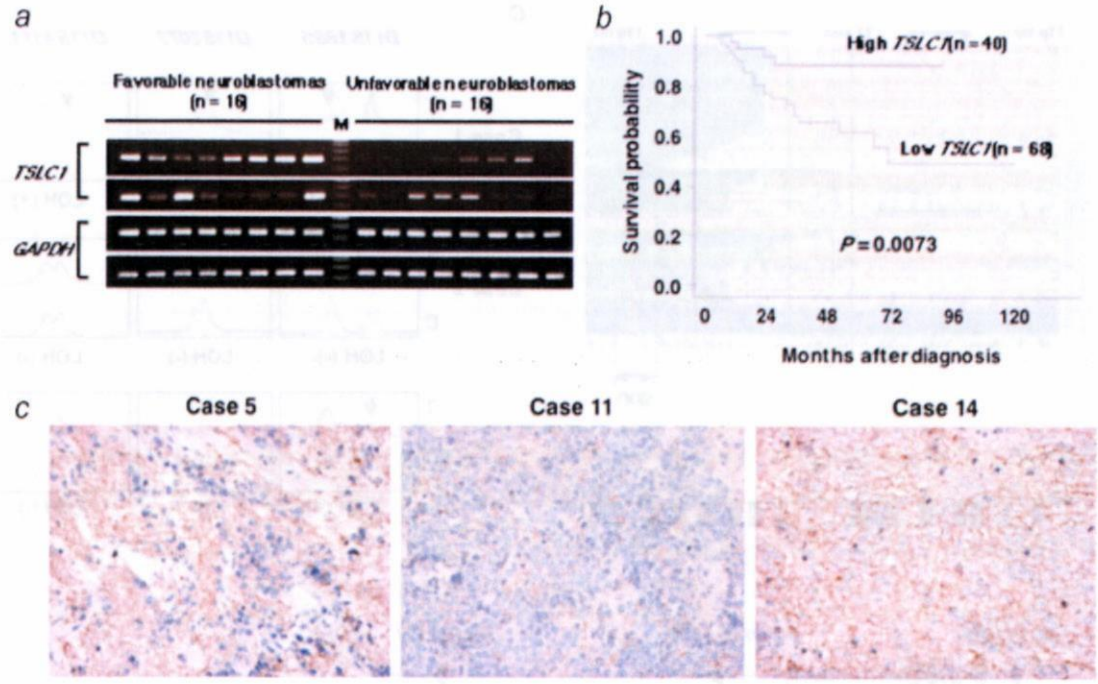

FIGURE 2 – Expression levels of *TSLC1* in primary neuroblastomas. (*a*) Expression of *TSLC1* in 16 favorable neuroblastomas bearing single copy of *MYCN* (Stage 1, higher expression levels of *TrkA*) and 16 unfavorable ones carrying *MYCN* amplification (stages 3 and 4, lower expression levels of *TrkA*). Total RNA was prepared from the indicated neuroblastoma tissues, reverse transcribed and amplified by PCR to examine the expression levels of *TSLC1*. *GAPDH* serves as an internal control. (*b*) Kaplan-Meier survival curves of patients with neuroblastomas based on higher or lower expression levels of *TSLC1*. Expression levels of *TSLC1* in 108 primary neuroblastoma samples categorized by their clinical stage were examined by a quantitative real-time PCR. Relative expression levels of *TSLC1* mRNA were determined by calculating the ratio between *GAPDH* and *TSLC1*. (*c*) Immunohistochemical analysis. Tumor samples derived from Case 5 (favorable neuroblastoma bearing single copy of *MYCN*), Case 11 (unfavorable neuroblastoma with *MYCN* amplification) and Case 14 (unfavorable neuroblastoma carrying single copy of *MYCN*) were fixed and stained with polyclonal anti-TSLC1 antibody.

primary neuroblastoma but not in neuroblastoma-derived cell lines.

Lower expression levels of TSLC1 are associated with poor outcome of neuroblastoma

To evaluate whether there could exist a possible relationship between *TSLC1* expression levels and clinicopathological factors of neuroblastoma patients, we have performed a quantitative real-time PCR. For this purpose, total RNA prepared from 108 primary neuroblastoma samples was subjected to a quantitative real-time PCR. According to the mean values of its expression levels obtained from a quantitative real-time PCR, these patients were divided into 2 groups including 40 patients with tumors expressing higher levels of *TSLC1* (High *TSLC1*) and 68 patients with tumors expressing lower levels of *TSLC1* (Low *TSLC1*). As shown in Table I, the significant differences were detectable between the above-mentioned 2 groups with respect to INSS stage, Shimada's pathological classification, copy number of *MYCN*, *TrkA* expression levels and DNA index. In contrast, no significant differences were observed between them with respect to their age, tumor origin and LOH on *TSLC1* locus.

We then examined whether there could exist a possible correlation between the expression levels of *TSLC1* in primary neuroblastomas and the survival of patients with neuroblastomas. The log-rank test showed that lower expression levels of *TSLC1* significantly correlate with unfavorable outcome ($p = 0.007$) as shown

TABLE I – CORRELATION BETWEEN *TSLC1* EXPRESSION AND OTHER PROGNOSTIC FACTORS OF NEUROBLASTOMA

Terms	*TSLC1* expression		*p*-Value
	High *TSLC1* ($n = 40$)	Low *TSLC1* ($n = 68$)	
Age (year)			
<1.5	23	29	
>1.5	17	39	0.1646
Tumor origin			
Adrenal grand	20	36	
Others	20	30	0.6915
Stage			
1, 2, 4S	24	25	
3, 4	16	43	0.0274
Shimada pathology			
Favorable	31	35	
Unfavorable	6	22	0.0227
MYCN copy number			
Single	38	51	
Amplified	2	17	0.0086
TrkA expression			
High	28	28	
Low	12	37	0.0090
DNA index			
Diploidy	8	39	
Aneuploidy	28	19	<0.0001
LOH			
(−)	18	29	
(+)	9	16	>0.9999

TABLE II – IMMUNOHISTOCHEMICAL ANALYSIS OF *TSLC1* EXPRESSION IN PRIMARY NEUROBLASTOMAS

Case	Age/Gender	*MYCN*	INPC	Primary site	Stage (INSS)	TSLC1
4	6 m/M	NA	NBL, Poorly diff., Low MKI, FH	Mediastinum	Stage 1	(+)
5	7 m/M	NA	NBL, Poorly diff., Low MKI, FH	Adrenal	Stage 1	(+)
6	9 m/M	NA	NBL, Poorly diff., Low MKI, FH	Adrenal	Stage 1	(+)
7	25 m/M	NA	NBL, Differentiating, Low MKI, FH	Adrenal	Stage 4	(+)
8	29 m/M	NA	NBL, Differentiating, Low MKI, FH	Mediastinum	Stage 2	(+)
9	13 m/M	A	NBL, Poorly diff., High MKI, UH	Adrenal	Stage 4	(−)
10	13 m/M	A	NBL, Poorly diff., Low MKI, UH	Abdominal	Stage 4	(−)
11	18 m/M	A	NBL, Poorly diff., Low MKI, UH	Adrenal	Stage 3	(−)
12	8 y/M	NA	NBL, Poorly diff., Low MKI, UH	Adrenal	Stage 4	(+)
13	8 m/M	NA	nGNB (NBL, poorly diff., Low MKI), UH	Mediastinum	Stage 2	(−)/(+)[1]
14	20 m/M	NA	NBL, Poorly diff., Low MKI, UH	Adrenal	Stage 3	(+)

m, months; y, years; M, male; NA, not amplified; A, amplified; NBL, neuroblastoma; nGNB, nodular ganglioneuroblastoma; MKI, mitosis-karyorrhexis index; FH, favorable histology; UH, unfavorable histology; (+), positive; (−), negative.
[1]Neuroblastoma component showed negative of TSLC1 signals, whereas ganglioneuroma showed positive of TSLC1 signals.

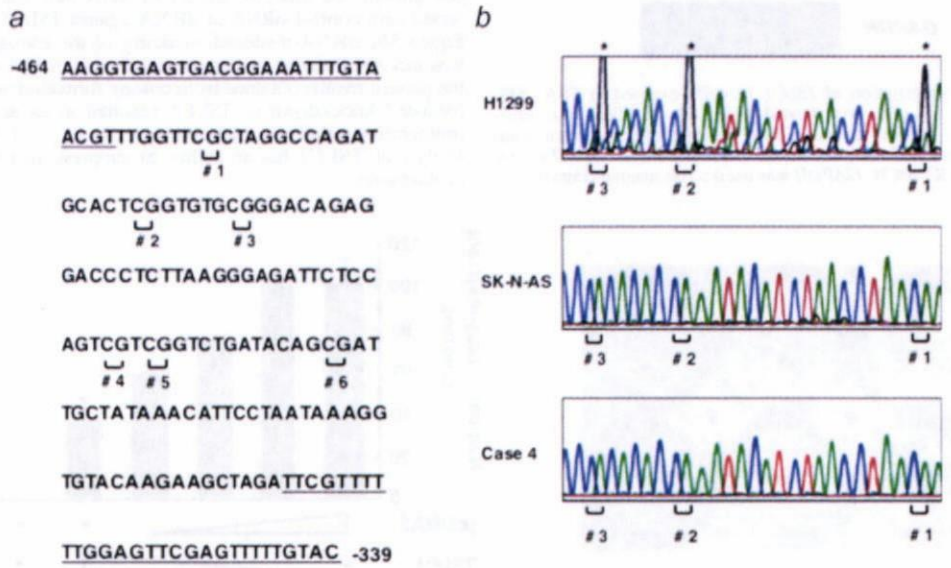

FIGURE 3 – Bisulfite-sequencing analysis of *TSLC1* gene promoter in neuroblastoma-derived cell lines and primary neuroblastomas. (*a*) Nucleotide sequence spanning from −464 to −339 relative to the translational initiation site (+1). Six CpG sites are shown. Primer sequences used for PCR-based amplification are underlined. (*b*) Bisulfite-sequencing analysis. Sequencing histograms showing the methylation status of CpG sites (#1, #2 and #3) are depicted. Asterisks indicate the positions of the methylated cytosine residues at the indicated CpG sites. H1299 cells were used as a positive control. [Color figure can be viewed in the online issue, which is available at www.interscience.wiley.com.]

in Kaplan-Meier cumulative survival curves (Fig. 2*b* and Supplementary Table I). Additionally, multivariable Cox analysis demonstrated that only clinical stage and *MYCN* amplification are significantly associated with their survival (Supplementary Table II), suggesting that *TSLC1* expression levels strongly correlate with these factors.

To further confirm the expression levels of TSLC1 in primary neuroblastomas, we employed immunohistochemical staining of TSLC1 in 11 primary neuroblastomas, including 5 favorable neuroblastomas bearing single copy of *MYCN*, 3 unfavorable neuroblastomas carrying single copy of *MYCN* and 3 unfavorable neuroblastomas with *MYCN* amplification. As shown in Figure 2*c*, TSLC1 appeared to be detectable at the cell–cell boundary of the tumors (cases 5 and 14) but not in Case 11. The immunohistochemical data were summarized in Table II. TSLC1 was detectable in tumors with favorable histology bearing single copy of *MYCN* (cases 4–8), whereas cases 9–11 with unfavorable histology carrying *MYCN* amplification did not express TSLC1. In addition, Case 13 was a nodular ganglioneuroblastoma whose ganglioneuroma and neuroblastoma components were TSLC1-positive and -negative, respectively. Of note, TSLC1 was detected in tumors with unfavorable histology bearing single copy of *MYCN* (cases 12–14). These observations indicate that there exists an inverse relationship between the expression levels of TSLC1 and *MYCN* amplification in primary neuroblastomas.

No promoter methylation of TSLC1 gene in neuroblastoma cell lines and primary neuroblastomas

Based on our present results, lower expression levels of *TSLC1* gene in unfavorable neuroblastomas might not be due to allelic loss of *TSLC1* locus. Since accumulating evidence strongly suggests that the downregulation of *TSLC1* in several cancers is associated with the hypermethylation of its promoter region,[9,11,12,24,26–29] we sought to examine whether the hypermethylation of *TSLC1* promoter region could be detectable in unfavorable neuroblastomas. For this purpose, we directly examined the methylation status of 6 cytosine residues of CpG sites within a putative *TSLC1* promoter region (Fig. 3*a*) by bisulfite-sequencing in 27 cell lines and 115 primary neuroblastomas. Sodium bisulfite modification of genomic DNA converts unmethylated cytosine residues to uracil residues but does not affect methylated cytosine residues. Unexpectedly, methylated cytosines

were undetectable in all primary neuroblastomas and cell lines, whereas hypermethylation was readily detected in human lung adenocarcinoma-derived H1299 cell line used as a positive control (Fig. 3*b*). Our present findings ruled out the possibility that the hypermethylation of *TSLC1* promoter region contributes to the downregulation of *TSLC1* gene in unfavorable neuroblastomas. Of note, the treatment of neuroblastoma-derived SH-SY5Y and CHP-134 cells with TSA (trichostatin A) resulted in a remarkable upregulation of *TSLC1* (Fig. 4). Since TSA is a histone deacetylase inhibitor, it is possible that the acetylation status of histone plays an important role in the regulation of *TSLC1* expression.

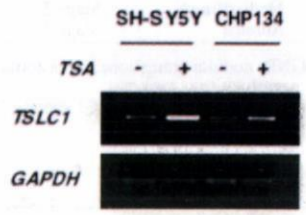

FIGURE 4 – Upregulation of *TSLC1* in cells exposed to TSA. SH-SY5Y and CHP-134 cells were treated with TSA (at a final concentration of 100 ng/ml) or left untreated. Twelve hours after treatment, total RNA was prepared and analyzed for the expression levels of *TSLC1* by semiquantitative RT-PCR. *GAPDH* was used as an internal control.

TSLC1 has an ability to suppress cell growth of neuroblastoma cells

To examine whether TSLC1 could have an ability to suppress neuroblastoma cell proliferation, we performed colony formation assays. Neuroblastoma-derived SH-SY5Y cells were transfected with or without the increasing amounts of the TSLC1 expression plasmid and maintained in fresh medium containing hygromycin for 14 days. As shown in Figure 5*a*, number of drug-resistant colonies was significantly reduced in a dose-dependent manner as compared with that in cells transfected with the empty plasmid alone. Similar results were also obtained in neuroblastoma-derived SK-N-AS cells (Supplementary Fig. 2). Next, we sought to examine a possible effect of the endogenous TSLC1 on neuroblastoma cell growth. To this end, SH-SY5Y cells were transiently transfected with control siRNA or siRNA against TSLC1. As shown in Figure 5*b*, siRNA-mediated silencing of the endogenous *TSLC1* was successful under our experimental conditions. Consistent with the present results obtained from colony formation assays, siRNA-mediated knockdown of TSLC1 resulted in an accelerated cell proliferation relative to the control cells ($p < 0.05$). Thus, it is likely that TSLC1 has an ability to suppress neuroblastoma cell proliferation.

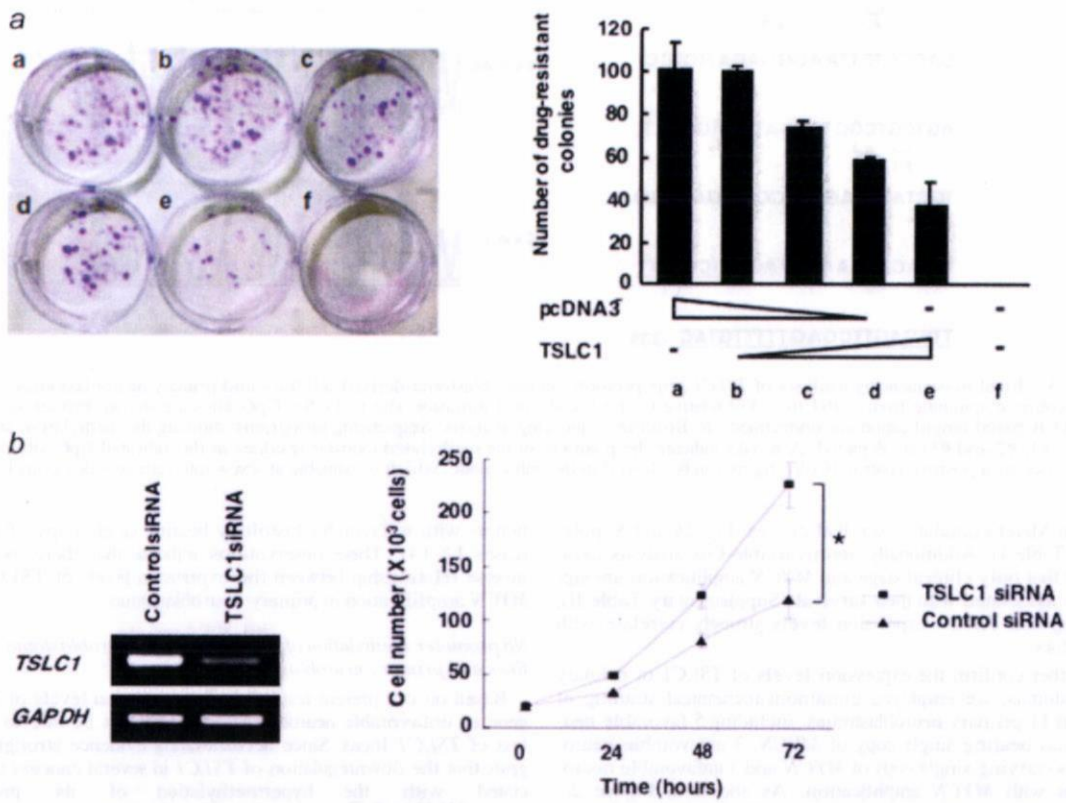

FIGURE 5 – Growth-suppressive potential of TSLC1 in neuroblastoma cells. (*a*) Colony formation assay. SH-SY5Y cells were transfected with the increasing amounts of the expression plasmid for TSLC1 (0, 250, 750 or 1,000 ng). Total amounts of plasmid DNA per transfection were kept constant (1 μg) with pcDNA3. Forty-eight hours after transfection, cells were transferred into the fresh medium containing hygromycin (at a final concentration of 200 μg/ml) and incubated for 2 weeks. Drug-resistant colonies were stained with Giemsa's solution (left panel) and number of drug-resistant colonies was scored (right panel). (*b*) siRNA-mediated knockdown of TSLC1. SH-SY5Y cells were transiently transfected with control siRNA or with siRNA against TSLC1. Forty-eight hours after transfection, total RNA was prepared and subjected to semiquantitative RT-PCR (left panel). At the indicated time periods after transfection, number of viable cells was measured in triplicate (right panel). The differences between the growth rate of control cells and TSLC1-knocked down cells were statistically significant ($p < 0.05$). [Color figure can be viewed in the online issue, which is available at www.interscience.wiley.com.]

Discussion

In the present study, we have demonstrated that the expression levels of a candidate tumor suppressor gene termed *TSLC1* are significantly associated with unfavorable outcome of patients with neuroblastomas. Our array-CGH studies revealed that *TSLC1* gene locates within the SRO of deletion in primary neuroblastoma at 11q. Indeed, its expression levels in primary neuroblastomas correlated with several prognostic indicators for neuroblastoma such as stage, Shimada's pathological classification, *MYCN* amplification status, *TrkA* expression levels and DNA index. Furthermore, TSLC1 had an ability to suppress neuroblastoma cell proliferation. Thus, it is likely that TSLC1 acts as a putative tumor suppressor for neuroblastoma.

As described previously, loss of *TSLC1* expression in primary esophageal squamous cell carcinoma (ESCC) preferentially correlated with invasion and metastasis,[12] and a remarkable reduction of *TSLC1* expression levels was observed in primary lung adenocarcinomas with advanced stage.[13] In addition, *TSLC1* expression was undetectable in 48% of benign (Grade I), 69% of atypical (Grade II) and 85% of anaplastic (Grade III) meningiomas.[14] Consistent with these observations, a significant downregulation of *TSLC1* was seen in unfavorable neuroblastomas bearing *MYCN* amplification as compared with favorable ones carrying single copy of *MYCN*, indicating that the decreased expression levels of *TSLC1* is one of the general properties of various human tumors including neuroblastoma. Intriguingly, there might exist an inverse relationship between the expression levels of *TSLC1* and *MYCN* amplification status in primary neuroblastoma. Indeed, our immunohistochemical analysis demonstrated that TSLC1 is detectable even in unfavorable neuroblastoma without *MYCN* amplification (Case 14). In a sharp contrast to primary neuroblastomas, the expression levels of *TSLC1* might be regulated in a *MYCN*-independent manner in neuroblastoma-derived cell lines. Although the precise molecular mechanisms behind the dysregulated expression of *TSLC1* in neuroblastoma cell lines, it might be due to certain genetic alterations occurred during the establishment of these cell lines.

Based on our present results, the presence of LOH at 11q was associated with unfavorable outcome of patients with neuroblastomas, however, there were no significant correlation between 11q LOH and the decreased expression levels of *TSLC1*. In accordance with these observations, the expression levels of *TSLC1* in neuroblastoma-derived cell lines were independent on their LOH status. These results suggest that the reduced expression levels of *TSLC1* in primary neuroblastomas are not attributed to haploinsufficiency. Alternatively, accumulating evidence strongly suggests that downregulation of *TSLC1* in various cancers including lung cancer, hepatocellular carcinoma, gastric cancer, pancreatic adenocarcinoma, prostate cancer, breast cancer, nasopharyngeal carcinoma and cervical cancer, might be due to the hypermethylation of its promoter region.[9,24–29] In a sharp contrast to these cancers, we did not detect the hypermethylation of the promoter region of *TSLC1* gene in primary neuroblastomas as well as neuroblastoma-derived cell lines under our experimental conditions. During the preparation of our article, Nowacki *et al*. found that there is no *TSLC1*-specific hypermethylation in neuroblastoma.[30] Similarly, the hypermethylation of *TSLC1* promoter region was not detectable in medulloblastoma.[31] According to the previous results, *RASSF1A* and *CASP8* gene promoters were frequently hypermethylated in primary neuroblastoma and neuroblastoma cell lines.[32] Thus, it is conceivable that, unlike the other cancers, hypermethylation of the promoter region of *TSLC1* does not contribute to its downregulation in neuroblastoma, and there might exist as yet unknown tissue-specific regulatory mechanisms of *TSLC1* transcription. Of note, the treatment of neuroblastoma-derived SH-SY5Y and CHP-134 cells with TSA (trichostatin A) resulted in a remarkable upregulation of *TSLC1*. Since TSA is a histone deacetylase inhibitor, it is likely that the acetylation status of histone plays an important role in the regulation of *TSLC1* expression. Further studies should be required to address this issue.

Several lines of evidence indicate that TSLC1 has an ability to delay the cell cycle progression.[12,16,33] Alternatively, enforced expression of TSLC1 resulted in an activation of proapoptotic caspase-3 and induction of proteolytic cleavage of its substrate PARP.[34] These findings strongly suggest that TSLC1 has an antiproliferative and/or proapoptotic activity. In a good agreement with this notion, our present results demonstrated that enforced expression of TSLC1 in SH-SY5Y cells as well as SK-N-AS cells decreases the number of drug-resistant colonies, and enforced depletion of the endogenous TSLC1 in SH-SY5Y cells leads to an accelerated cell proliferation, which was consistent with the recent observations.[30] Collectively, our present findings suggest that TSLC1 acts as a tumor suppressor for neuroblastoma, and also might contribute to the spontaneous regression of neuroblastoma arising from neuronal apoptosis and/or differentiation.

Acknowledgements

We thank institutions and hospitals for providing us tumor specimens. We are grateful to Drs. D.G. Albertson, D. Pinkel, B.G. Feuerstein, N. Tomioka, S. Oba and S. Ishii for their help to array CGH analysis. We also thank Mr. H. Kageyama, Dr. K. Koide, Dr. E. Isogai, Ms. N. Kitabayashi and Ms. Y. Nakamura for their excellent technical assistance. Dr. K. Ando is an awardee of Research Resident Fellowship from the Foundation for Promotion of Cancer Research (Japan) for the 3rd Term Comprehensive 10-Year Strategy for Cancer Control in Japan.

References

1. Evans AE, Gerson J, Schnaufer L. Spontaneous regression of neuroblastoma. Natl Cancer Inst Monogr 1976;44:49–54.
2. Brodeur GM. Neuroblastoma: biological insights into a clinical enigma. Nat Rev Cancer 2003;3:203–16.
3. Tomioka N, Oba S, Ohira M, Misra A, Fridlyand J, Ishii S, Nakamura Y, Isogai E, Hirata T, Yoshida Y, Todo S, Kaneko Y, et al. Novel risk stratification of patients with neuroblastoma by genomic signature which is independent of molecular signature. Oncogene 2008;27:441–9.
4. Guo C, White PS, Weiss MJ, Hogarty MD, Thompson PM, Stram DO, Gerbing R, Matthay KK, Seeger RC, Brodeur GM, Maris JM. Allelic deletion at 11q23 is common in MYCN single copy neuroblastomas. Oncogene 1999;18:4948–57.
5. Attiyeh EF, London WB, Mossé YP, Wang Q, Winter C, Khazi D, McGrady PW, Seeger RC, Look AT, Shimada H, Brodeur GM, Cohn SL, et al. Chromosome 1p and 11q deletions and outcome in neuroblastoma. N Engl J Med 2005;353:2243–53.
6. Mosse Y, Greshock J, King A, Khazi D, Weber BL, Maris JM. Identification and high-resolution mapping of a constitutional 11q deletion in an infant with multifocal neuroblastoma. Lancet Oncol 2003;4:769–71.
7. De Preter K, Vandesompele J, Menten B, Carr P, Fiegler H, Edsjö A, Carter NP, Yigit N, Waelput W, Van Roy N, Bader S, Pahlman S, et al. Positional and functional mapping of a neuroblastoma differentiation gene on chromosome 11. BMC Genomics 2005;6:97.
8. Wang Q, Diskin S, Rappaport E, Attiyeh E, Mosse Y, Shue D, Seiser E, Jagannathan J, Shusterman S, Bansal M, Khazi D, Winter C, et al. Integrative genomics identifies distinct molecular classes of neuroblastoma and shows that multiple genes are targeted by regional alterations in DNA copy number. Cancer Res 2006;66:6050–62.
9. Kuramochi M, Fukuhara H, Nobukuni T, Kanbe T, Maruyama T, Ghosh HP, Pletcher M, Isomura M, Onizuka M, Kitamura T, Sekiya T, Reeves RH, et al. TSLC1 is a tumor suppressor gene in human non-small-cell lung cancer. Nat Genet 2001;27:427–30.
10. Masuda M, Yageta M, Fukuhara H, Kuramochi M, Maruyama T, Nomoto A, Murakami Y. The tumor suppressor protein TSLC1 is involved in cell-cell adhesion. J Biol Chem 2002;277:31014–19.
11. Fukami T, Fukuhara H, Kuramochi M, Maruyama T, Isogai K, Sakamoto M, Takamoto S, Murakami Y. Promoter methylation of TSLC1 gene in advanced lung tumors and various cancer cell lines. Int J Cancer 2003;107:53–9.
12. Ito T, Shimada Y, Hashimoto Y, Kaganoi J, Kan T, Watanabe G, Murakami Y, Imamura M. Involvement of TSLC1 in progression of esophageal squamous cell carcinoma. Cancer Res 2003;653:6320–6.

13. Uchino K, Ito A, Wakayama T, Koma Y, Okada T, Ohbayashi C, Iseki S, Kitamura Y, Tsubota N, Okita Y, Okada M. Clinical implication and prognostic significance of the tumor suppressor TSLC1 gene detected in adenocarcinoma of the lung. Cancer 2003;98:1002–7.
14. Surace EI, Lusis E, Murakami Y, Scheithauer BW, Perry A, Gutmann DH. Loss of tumor suppressor in lung cancer-1 (TSLC1) expression in meningioma correlates with increased malignancy grade and reduced patient survival. J Neuropathol Exp Neurol 2004;63:1015–27.
15. Houshmandi SS, Surace EI, Zhang HB, Fuller GN, Gutmann DH. Tumor suppressor in lung cancer-1 (TSLC1) functions as a glioma tumor suppressor. Neurology 2006;67:1863–6.
16. Lung HL, Cheung AK, Xie D, Cheng Y, Kwong FM, Murakami Y, Guan XY, Sham JS, Chua D, Protopopov AI, Zabarovsky ER, Tsao SW, et al. TSLC1 is a tumor suppressor gene associated with metastasis in nasopharyngeal carcinoma. Cancer Res 2006;66:9385–92.
17. Brodeur GM, Pritchard J, Berthold F, Carlsen NL, Castel V, Castelberry RP, Bernardi BD, Evans AE, Favrot M, Hedborg F. Revisions of the international criteria for neuroblastoma diagnosis, staging, and response to treatment. J Clin Oncol 1993;11:1466–77.
18. Kaneko M, Tsuchida Y, Uchino J, Takeda T, Iwafuchi M, Ohnuma N, Mugishima H, Yokoyama J, Nishihira H, Nakada K, Sasaki S, Sawada T, et al. Treatment results of advanced neuroblastoma with the first Japanese study group protocol. Study Group of Japan for Treatment of Advanced Neuroblastoma. J Pediatr Hematol Oncol 1999;21:190–7.
19. Kaneko M, Nishihira H, Mugishima H, Ohnuma N, Nakada K, Kawa K, Fukuzawa M, Suita S, Sera Y, Tsuchida Y. Stratification of treatment of stage 4 neuroblastoma patients based on N-myc amplification status. Med Pediatr Oncol 1998;31:1–7.
20. Ohira M, Morohashi A, Inuzuka H, Shishikura T, Kawamoto T, Kageyama H, Nakamura Y, Isogai E, Takayasu H, Sakiyama S, Suzuki Y, Sugano S, et al. Expression profiling and characterization of 4200 genes cloned from primary neuroblastomas: identification of 305 genes differentially expressed between favorable and unfavorable subsets. Oncogene 2003;22:5525–36.
21. Misra A, Pellarin M, Shapiro J, Feuerstein BG. A complex rearrangement of chromosome 7 in human astrocytoma. Cancer Genet Cytogenet 2004;151:162–70.
22. Jain AN, Tokuyasu TA, Snijders AM, Segraves R, Albertson DG, Pinkel D. Fully automatic quantification of microarray image data. Genome Res 2002;12:325–32.
23. Kikuchi S, Yamada D, Fukami T, Maruyama T, Ito A, Asamura H, Matsuno Y, Onizuka M, Murakami Y. Hypermethylation of the *TSLC1/IGSF4* promoter is associated with tobacco smoking and a poor prognosis in primary non-small cell lung carcinoma. Cancer 2006;106:1751–8.
24. Fukuhara H, Kuramochi M, Fukami T, Kasahara K, Furuhata M, Nobukuni T, Maruyama T, Isogai K, Sekiya T, Shuin T, Kitamura T, Reeves RH, et al. Promoter methylation of TSLC1 and tumor suppression by its gene product in human prostate cancer. Jpn J Cancer Res 2002;93:605–9.
25. Hui AB, Lo KW, Kwong J, Lam EC, Chan SY, Chow LS, Chan AS, Teo PM, Huang DP. Epigenetic inactivation of TSLC1 gene in nosopharyngeal carcinoma. Mol Carcinog 2003;38:170–8.
26. Honda T, Tamura G, Waki T, Jin Z, Sato K, Motoyama T, Kawata S, Kimura W, Nishizuka S, Murakami Y. Hypermethylation of the TSLC1 gene promoter in primary gastric cancers and gastric cancer cell lines. Jpn J Cancer Res 2002;93:857–60.
27. Steenbergen RD, Kramer D, Braakhuis BJ, Stern PL, Verheijen RH, Meijer CJ, Snijders PJ. TSLC1 gene silencing in cervical cancer cell lines and cervical neoplasia. J Natl Cancer Inst 2004;96:294–305.
28. Jansen M, Fukushima N, Rosty C, Walter K, Altink R, Heek TV, Hruban R, Offerhaus JG, Goggins M. Abberant methylation of 5′ CpG island of TSLC1 is common in pancreatic ductal adenocarcinoma and is first manifest in high-grade PanINs. Cancer Biol Ther 2002;1:293–6.
29. Allinen M, Peri L, Kujala S, Lahti-Domenici J, Outila K, Karppinen SM, Launonen V, Winqvist R. Analysis of 11q21–24 loss of heterozygosity candidate target genes in breast cancer: indications of *TSLC1* promoter hypermethylation. Genes Chromosomes Cancer 2002;34:384–9.
30. Nowacki S, Skowron M, Oberthuer A, Fagin A, Voth H, Brors B, Westermann F, Eggert A, Hero B, Berthold F, Fischer M. Expression of the tumor suppressor gene TSLC1 is associated with favorable outcome and inhibits cell survival in neuroblastoma. Oncogene 2008;27:3329–38.
31. Lindsey JC, Lusher ME, Anderton JA, Bailey S, Gilbertson RJ, Pearson AD, Ellison DW, Clifford SC. Identification of tumor-specific epigenetic in medulloblastoma development by hypermethylation profiling. Carcinogenesis 2004;25:661–8.
32. Lázcoz P, Muñoz J, Nistal M, Pestaña A, Encío I, Castresana JS. Frequent promoter hypermethylation of RASSF1A and CASP8 in neuroblastoma. BMC Cancer 2006;6:254.
33. Sussan TE, Pletcher MT, Murakami Y, Reeves RH. Tumor suppressor in lung cancer 1 (TSLC1) alters tumorigenic growth properties and gene expression. Mol Cancer 2005;4:28.
34. Mao X, Seidlitz E, Truant R, Hitt M, Ghosh HP. Re-expression of TSLC1 in a non-small-cell lung cancer cell line induces apoptosis and inhibits tumor growth. Oncogene 2004;23:5632–42.

blood
2008 111: 776-784
Prepublished online Sep 21, 2007;
doi:10.1182/blood-2007-05-088310

Molecular allelokaryotyping of pediatric acute lymphoblastic leukemias by high-resolution single nucleotide polymorphism oligonucleotide genomic microarray

Norihiko Kawamata, Seishi Ogawa, Martin Zimmermann, Motohiro Kato, Masashi Sanada, Kari Hemminki, Go Yamatomo, Yasuhito Nannya, Rolf Koehler, Thomas Flohr, Carl W. Miller, Jochen Harbott, Wolf-Dieter Ludwig, Martin Stanulla, Martin Schrappe, Claus R. Bartram and H. Phillip Koeffler

Blood (print ISSN 0006-4971, online ISSN 1528-0020), is published semimonthly by the American Society of Hematology, 1900 M St, NW, Suite 200, Washington DC 20036.

Molecular allelokaryotyping of pediatric acute lymphoblastic leukemias by high-resolution single nucleotide polymorphism oligonucleotide genomic microarray

Norihiko Kawamata,[1] Seishi Ogawa,[2] Martin Zimmermann,[3] Motohiro Kato,[2] Masashi Sanada,[2] Kari Hemminki,[4] Go Yamatomo,[2] Yasuhito Nannya,[2] Rolf Koehler,[5] Thomas Flohr,[5] Carl W. Miller,[1] Jochen Harbott,[6] Wolf-Dieter Ludwig,[7] Martin Stanulla,[3] Martin Schrappe,[8] Claus R. Bartram,[5] and H. Phillip Koeffler[1]

[1]Department of Hematology, Oncology, Cedars-Sinai Medical Center/University of California at Los Angeles School of Medicine; [2]Regeneration Medicine of Hematopoiesis, University of Tokyo, School of Medicine, Tokyo, Japan; [3]Department of Pediatric Hematology and Oncology, Children's Hospital, Hannover Medical School (MHH), Hannover, Germany; [4]Division of Molecular Genetic Epidemiology, German Cancer Research Center (DKFZ), Heidelberg, Germany; [5]Institute of Human Genetics, University of Heidelberg, Heidelberg, Germany; [6]Department of Pediatric Hematology and Oncology, Justus Liebig University, Gießen, Germany; [7]Department of Hematology, Oncology and Tumor Immunology, Robert-Rössle-Clinic at the HELIOS-Clinic Berlin-Buch, Charité, Berlin, Germany; and [8]Department of Pediatrics, University of Kiel, Kiel, Germany

Pediatric acute lymphoblastic leukemia (ALL) is a malignant disease resulting from accumulation of genetic alterations. A robust technology, single nucleotide polymorphism oligonucleotide genomic microarray (SNP-chip) in concert with bioinformatics offers the opportunity to discover the genetic lesions associated with ALL. We examined 399 pediatric ALL samples and their matched remission marrows at 50 000/250 000 SNP sites using an SNP-chip platform. Correlations between genetic abnormalities and clinical features were examined. Three common genetic alterations were found: deletion of *ETV6*, deletion of *p16INK4A*, and hyperdiploidy, as well as a number of novel recurrent genetic alterations. Uniparental disomy (UPD) was a frequent event, especially affecting chromosome 9. A cohort of children with hyperdiploid ALL without gain of chromosomes 17 and 18 had a poor prognosis. Molecular allelokaryotyping is a robust tool to define small genetic abnormalities including UPD, which is usually overlooked by standard methods. This technique was able to detect subgroups with a poor prognosis based on their genetic status. (Blood. 2008;111:776-784)

Introduction

Pediatric acute lymphoblastic leukemia (ALL) is the most common malignant disease in children.[1-3] ALL is a genetic disease resulting from accumulation of mutations of tumor suppressor genes and oncogenes.[1-3] Knowledge of these mutations can be of use for diagnosis, prognosis, and therapeutic clinical purposes, as well as to provide an overall understanding of the pathogenesis of ALL.[1-3] Identification of mutated genes in ALL has evolved with improvement in technology. A recent approach is single nucleotide polymorphism (SNP) analysis using an array-based technology[4,5] that allows identification of amplifications, deletions, and allelic imbalance, such as uniparental disomy (UPD [represents the doubling of the abnormal allele due to somatic recombination or duplication and loss of the other normal allele]).[6-8] However, since this technique detects allelic dosage, it cannot detect balanced translocations.

According to the HapMap publication, 9.2 million SNPs have been reported, and of these, 3.6 million have been validated.[9] Global genomic distribution of SNPs and its easy adaptability for high throughput analysis make them the target of choice to look for genomic abnormalities in ALL and other cancers.[5-7]

Recently, higher resolution SNP-chip (50 000-500 000 probes) has been developed for large-scale SNP typing.[4,10] With a large number of SNP probes, in combination with the algorithms specifically developed for copy number calculations, these SNP-chips enable genomewide detection of copy number changes.[11,12] The combination of SNP-chip technology, nucleotide sequencing, and bioinformatics allows the investigator to view the entire genome of ALL in an unbiased, comprehensive approach. Using SNP-chips, the chromosomal abnormalities can be evaluated at a very high resolution (molecular level: average distances of each probe are 47 kb and 5.8 kb in the 50 k/500 k arrays, respectively[4,10]), and allele-specific gene dosage level (gene dosage of paternal and maternal alleles) also can be analyzed in the whole genome.[11,12] Hence, we name this new technology "molecular allelokaryotyping."[12] In this study, we performed molecular allelokaryotyping on a very large cohort (399) of pediatric ALL samples to examine genomic abnormalities at high resolution. Further, we examined correlations between the genomic abnormalities detected by SNP-chip and clinical features, including prognosis.

Submitted May 1, 2007; accepted September 13, 2007. Prepublished online as *Blood* First Edition paper, September 21, 2007; DOI 10.1182/blood-2007-05-088310.

N.K., S.O., and M.Z. equally contributed to this work as first authors. C.R.B. and H.P.K. equally contributed to this work as last authors.

An Inside *Blood* analysis of this article appears at the front of this issue.

The online version of this article contains a data supplement.

The publication costs of this article were defrayed in part by page charge payment. Therefore, and solely to indicate this fact, this article is hereby marked "advertisement" in accordance with 18 USC section 1734.

Methods

Clinical samples and DNA/RNA preparation

The ALL-BFM 2000 trial of the Berlin-Frankfurt-Münster (BFM) study group on treatment of childhood ALL enrolled patients from ages 1 year to 18 years at diagnosis.

From September 1999 to January 2002, 566 patients were consecutively enrolled in this trial. The ALL-BFM 2000 study was approved by the ethics committees of the Medical School Hanover and the Cedar Sinai Medical Center. Informed consent was obtained in accordance with the Declaration of Helsinki.

Of the 566 patients (nos. 299-854), 399 patients, representing 70% of the entire patient population, had additional DNA available and could be included in the present SNP-chip study. The 167 patients not available for this analysis did not differ from the 399 patients in this study with regard to their clinical and biological characteristics (data not shown).

Complete remission (CR) was defined as the absence of leukemia blasts in the peripheral blood and cerebrospinal fluid, fewer than 5% lymphoblasts in marrow aspiration smears, and no evidence of localized disease. At day 29, bone marrows were examined, and all patients in this SNP-chip analysis study obtained a CR at that time. The remission marrows were collected and used as matched control for the SNP-chip analysis.

Prednisone response was defined based on numbers of peripheral blood blasts per microliter on day 8, and patients were classified into good (< 1000 blasts/μL) and poor responders (≥ 1000 blasts/μL).[13-15] Relapse was defined as recurrence of lymphoblasts or localized leukemic infiltrates at any site.

DNA index, immunophenotyping, molecular analysis of chromosomal abnormalities

Leukemic or normal bone marrow cells were stained with propidium iodide, and cellular DNA contents were measured by cytometric analysis as previously reported.[16,17] DNA index was defined as the DNA content of leukemic cells compared with normal G0/G1 cells. When the DNA index of leukemic cells was the same as or greater than 1.16, it was defined as hyperdiploid ALL by DNA index as previously reported.[16,17]

Immunophenotyping of ALL was examined using anti-CD2, -CD3, -CD4, -CD10, -CD19, and -CD20 antibodies by FACS.[13-15] ETV6/RUNX1, BCR/ABL, and MLL/AF4 were examined by interphase fluorescence in situ hybridization (FISH) analysis using specific probes and by reverse transcriptase–polymerase chain reaction (RT-PCR) using specific primers for these fusion transcripts as described previously.[13-15]

Molecular allelokaryotyping of leukemic cells

DNA from the 399 ALL samples as well as their paired normal DNA from remission samples were analyzed on Affymetrix GeneChip human mapping 50 K *Xba*I or 250 K Nsp arrays (Affymetrix Japan, Tokyo, Japan) according to the manufacturer's protocol. Microarray data were analyzed for determination of both total and allelic-specific copy numbers using the CNAG program as previously described[11,12] with minor modifications, where the status of copy numbers as well as UPD at each SNP was inferred using the algorithms based on Hidden Markov Models.[11,12]

For clustering of ALL samples with regard to the status of copy number changes as well as UPD, entire genome was divided into contiguous sub-blocks of 100 kb in length, and according to the inferred copy numbers (CNs) and the status of UPD, one of the 4 conditions was assigned to the *i*th sub-block (*Si*); CN gain, CN loss, normal CN, and UPD. For a given 2-copy number data, A and B, distance (d[A,B])was simply defined as

$$d(A,B) = \sum_i \mathrm{I}(S_i^A; S_i^B)$$

$$\mathrm{I}(S_i^A; S_i^B) = \begin{cases} 1 \text{ if } S_i^A = S_i^B \\ 0 \text{ if } S_i^A \neq S_i^B \end{cases}$$

where S_i^A and S_i^B are the status of the *i*th sub-block (*Si*) in data A and B, respectively, and sum is taken for all sub-blocks. Clustering was initiated by finding a seed cluster of 2 samples showing the minimum distance and replacing them with the cluster data having the mean *Si* value of the two. This procedure was iteratively performed until all samples were converged to one cluster based on this distance using a program developed for this purpose (GNAGraph), which was followed by manual revisions focusing on particular genetic lesions selected by their frequencies within the sample set. CNAG and CNAGraph are available on request.

Quantitative genomic PCR and direct sequencing

Quantitative genomic PCR (qPCR) was performed on a real-time PCR machine, iCycler (Bio-Rad Laboratories, Hercules, CA) using iQ cybergreen supermix (Bio-Rad Laboratories) according to the manufacturer's protocol. Primer sequences used for the qPCR are listed in Table S2 (available on the *Blood* website; see the Supplemental Materials link at the top of the online article). Gene dosage at the 2p allele was used as an internal control. Allelic gene dosage of 9p and 9q was measured, and these were compared with the levels in respective matched control DNA. SNP sites were amplified and directly sequenced on Autosequencer 3000 (Applied Biosystems, Foster City, CA). Primers used for SNP site amplification are listed in Table S2. Exons 12 and 14 of JAK2 gene were amplified as previously reported.[18] PCR products were purified and subjected to direct sequencing.

Data preparation

Proportional differences between groups were analyzed by either chi-squared (χ^2) or Fisher exact tests. The Kaplan-Meier method was used to

Table 1. Characterization of clinical features of 399 ALL cases

	Cases, no. (%)
Sex	
Male	230 (57)
Female	169 (43)
Age	
1 to 9 yrs	307 (77)
Older than 10 yrs	92 (23)
WBC	
Below $10^2 \times 10^9$/L	362 (91)
Over $10^2 \times 10^9$/L	37 (9)
Immunophenotype	
T-cell	49 (12)
B-cell	339 (85)
Unknown	11 (3)
CNS involvement	
Yes	11 (3)
No	358 (90)
unknown	30 (7)
BCR/ABL	
Yes	6 (2)
No	379 (95)
Unknown	14 (3)
ETV6/RUNX1	
Yes	96 (24)
No	270 (68)
Unknown	33 (8)
PDN response	
Good	360 (90)
Poor	35 (9)
Unknown	4 (1)

WBC indicates white blood cell count ($\times 10^9$/L) in peripheral blood at diagnosis; CNS involvement, central nervous system involvement at diagnosis; *BCR/ABL* and *ETV6/RUNX1*, *BCR/ABL* or *ETV6/RUNX1* fusion was examined by RT-PCR and/or FISH analysis; PDN, prednisone; and PDN response, blast cell count was 1000/μL or greater in peripheral blood after a 7-day exposure to prednisone and one intrathecal dose of methotrexate.

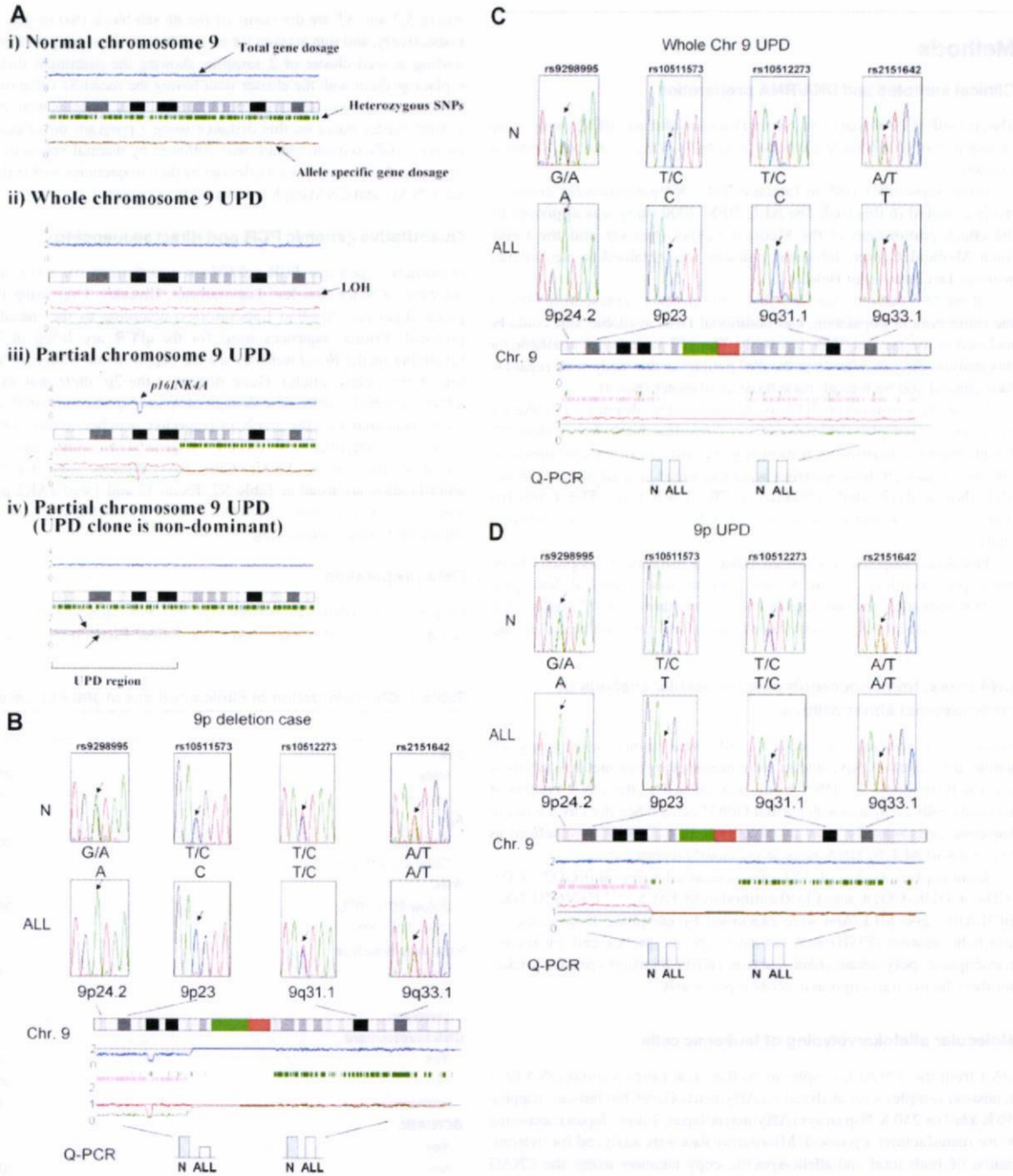

Figure 1. Result of SNP-chip analysis. (A) Results of normal and abnormal chromosomes visualized by CNAG software. Blue lines above each chromosome show total gene dosage; level 2 indicates diploid (2N) amount of DNA, which is normal. Green bars under each chromosome indicate the SNP sites showing heterozygosity in leukemic cells. When heterozygosity is not detected in the leukemic cells but is detected in matched normal controls, the result suggests that the leukemic cells have allelic imbalance (AI) in that region. Pink bars that replaced green ones suggest AI. The bottom lines (green and red lines) in each panel show allele-specific gene dosage levels (one indicates the gene dosage of paternal allele, the other indicates the gene dosage of maternal allele). Level 1 is normal for each gene dosage. (i) Pattern of normal chromosome 9. Blue line is at level 2 (2N DNA). Large number of SNP sites shows normal heterozygosity (green bars under the chromosomes), and no pink bars are detected. Allele-specific gene dosage is at level 1. Panel ii shows the pattern of whole chromosome 9 uniparental disomy (UPD) detected by SNP-chip. Total gene dosage (blue line) is normal (level 2). A number of pink bars (AI) are detected. Allele-specific gene dosage data show that one allele is deleted (level 0) and the other allele is duplicated (level 2). Panel iii shows the pattern of partial UPD. Left half shows the pattern of UPD as described above. Right half shows the pattern of a normal chromosome as described above. This case also has homozygous deletion of *p16INK4A* gene (see that both allele-specific dosage lines [green and red lines] and total gene dosage line [blue line] are at zero). Panel iv shows nondominant UPD. Total gene dosage (blue line) indicates 2N. Allele-specific gene dosage lines (arrows, green and red lines) on left half show that one allele (green line) is lower than normal, and the other allele (red line) is higher than normal. Allele-specific gene dosage on right half show that each allele has same level. (B-D) Validation of SNP-chip data by direct nucleotide sequencing of SNP sites and qPCR. Top panels: direct nucleotide sequencing of SNP sites in ALL samples with matched controls. ALL indicates leukemic samples; N, matched control samples. Heterozygous SNP sites are indicated by arrows. Middle panels: results of SNP-chip data (see Figure 1 legend). Bottom panels: qPCR at each chromosome location. Gene dosage levels were examined using qPCR at indicated chromosomal region. Gene dosage was determined relative to the levels at the 2p21 region. Gene dosage in leukemic cells (ALL) was compared with the matched normal control DNA (N). (B) ALL with 9p hemizygous deletion; homozygous deletion of 9p21 is also detected. (C) ALL with whole chromosome UPD. (D) ALL with 9p UPD.